Design and fabrication of a miniature spectrometer-on-a-chip for Biodiesel sensing applications

Alvaro Casas Bedoya

Promotor(s)/Supervisor(s): dr. ir. Dries Van Thourhout

Assisting supervisor(s): Joost Brouckaert, Nebiyu A Yebo

Master dissertation submitted in order to obtain the academic degree of

Erasmus Mundus Master of Science in Photonics

Academic year 2008-2009

UNIVERSITEIT GENT

Vrije Universiteit Brussel

KTH VETENSKAP OCH KONST ROYAL INSTITUTE OF TECHNOLOGY

HERIOT WATT UNIVERSITY

University of St Andrews

Design and fabrication of a miniature spectrometer-on-a-chip for Biodiesel sensing applications

Alvaro Casas Bedoya

Promotor: prof. dr. ir. Dries Van Thourhout
Begeleider I : Ir. Joost Brouckaert
Begeleider II: Ir. Nebiyu A Yebo

Masterproef ingediend tot het behalen van de academische graad van
Erasmus Mundus Master of Science in Photonics

Vakgroep Informatietechnologie
Voorzitter: prof. dr. ir. Daniël De Zutter
Faculteit Ingenieurswetenschappen
Academiejaar 2008-2009

UNIVERSITEIT GENT

Toelating tot bruikleen

De auteur geeft de toelating dit afstudeerwerk voor consultatie beschikbaar te stellen en delen van het afstudeerwerk te copieren voor persoonlijk gebruik. Elk ander gebruik valt onder de beperkingen van het auteursrecht, in het bijzonder met betrekking tot de verplichting de bron uitdrukkelijk te vermelden bij het aanhalen van resultaten uit dit afstudeerwerk.

Permission for usage (English version)

The author gives his permission to make this work available for consultation and to copy part of the work for personal use. Any other use is bound to the restriction of copyright legislation, in particular regarding the obligation to specify the source when using results of this work.

Alvaro Casas Bedoya

1st June 2009

Acknowledgements

I would like to take this opportunity to thank all the people who contributed to my professional development in the past two years:

The support and funding of EMMP consortium was invaluable for this project. Special thanks to Dr. Irina Veretennicoff.

In St Andrews, I would like to thank to Dr. Bruce D. Sinclair and his family, for their assistance during the transition between countries and for show me his big commitment and energy to work. I would also like to thank Dr. Thomas F. Krauss for his invaluable guidance and for his assistance with my professional growth. In Gent I would like to thank to Dr. Roel Baets, for his nice welcome and his example of leadership.

Also thanks to Bert Coryn and Dave Steyaert, for all the solved question. Very special thanks to Shankar Kumar Selvaraja, Steven Verstuyft, Pieter Dumon and Wim Bogaerts, for all their time, support and instruction during my thesis year in Gent.

My gratitude also goes to Nebiyu A. Yebo for his patience and assistance in the final stage of my work. I want to express also my sincere gratitude to my supervisor Joost Brouckeart, for his advice, wisdom, and understanding, but most of all for his unwavering dedication and his expert advice during the completion of my thesis project.

Thanks to my promotor Dr. Dries Van Thourhout, for believing in me from the beginning and his encouragement of my academic explorations.

Most important, I want to thank God for all the blessing received.

Finally, I want to thank my wife Carolina for her unconditional love, friendship and support during these two years, also my gratitude and love goes to my parents Alvaro and Luz Mary, my sisters Carolina, Adriana and Claudia, and all my family, for their unwavering love and encouragement during each stage of my career.

Thank you all!

Abstract

By measuring the transmission of Biodiesel/Diesel mixtures in the near- and far-infrared wavelength ranges, it is possible to predict the blend level with a high accuracy. Conventional photospectrometers are typically large and expensive and have a performance that often exceeds the requirements for most applications. For automotive applications for example, what counts is size, robustness and most important cost. As a result the miniaturization of the spectrometer can be seen as an attractive implementation of a Biodiesel sensor.

Using Silicon-on-Insulator (SOI) this spectrometer miniaturization can be achieved. Due to the large refractive index contrast of the SOI material system, photonic devices can be made very compact. Moreover, they can be manufactured on high-quality SOI substrates using waferscale CMOS fabrication tools, making them cheap for the market.

In this work, we show that it is possible to determine Biodiesel blend levels using an SOI spectrometer-on-a-chip. We demonstrate absorption measurements using spiral shaped waveguides and we also present the spectrometer designed and fabricated for on-chip Biodiesel/Diesel blend measurements.

Keywords: Silicon-on-Insulator, Planar concave demultiplexer, Biodiesel/Diesel blends measurement.

Biodiesel sensing using Silicon-on-Insulator technologies

Alvaro Casas Bedoya

Supervisors: ir. Joost Brouckaert and ir. Nebiyu A Yebo. Promoter: Prof. Dr. ir. Dries Van Thourhout

ABSTRACT

By measuring the transmission of Biodiesel/Diesel mixtures in the near- and far-infrared wavelength ranges, it is possible to predict the blend level with a good accuracy. Conventional photospectrometers are typically large and expensive and have a performance that often exceeds the requirements for most applications. For automotive applications for example, what counts is size, robustness and most important cost. As a result the miniaturization of the spectrometer can be seen as an attractive implementation of a Biodiesel sensor.

Using Silicon-on-Insulator (SOI) this spectrometer miniaturization can be achieved. Due to the large refractive index contrast of the SOI material system, photonic devices can be made very compact. Moreover, they can be manufactured on high-quality SOI substrates using waferscale CMOS fabrication tools, making them cheap for the market.

In this paper, we show that it is possible to determine Biodiesel blend levels using an SOI spectrometer-on-a-chip. We demonstrate absorption measurements using spiral shaped waveguides and we also present the spectrometer design for on-chip Biodiesel blend measurements.

Keywords: Silicon-on-Insulator, Planar concave demultiplexer, Biodiesel/Diesel blends measurement.

1. INTRODUCTION

Biodiesel is a biofuel with methyl esters as a primary compound. These can be produced from different types of biomass, including animal fats, waste cooking oil and oilseed rape. Oilseed rape, in particular, is one of the principal sources of biofuel because it can be cultivated on a fairly wide range of agricultural land. Biofuel has become potentially important because it is a nontoxic, biodegradable and renewable source of energy that, in contrast to conventional Diesel fuel [2] reduces the carbon dioxide (CO_2) emission in a combustion process.

A planar concave grating (PCG) is an interesting wavelength filter used as a miniaturized spectrometer, due to its possible small size, high resolution and large channel count. These devices have been realized in many material systems including silica-on-silicon, III–V's, large core silicon-on-insulator (SOI) substrates [7] and nanophotonic SOI substrates [8; 9]. This last one is a promising material system for a wide range of applications, such as telecommunications and optical sensors. Due to the large omnidirectional index contrast of this material system, these devices can be made very compact and they can be manufactured on high-quality SOI substrates using CMOS fabrication tools, making these devices cheap for the market.

In this paper, we demonstrate the feasibility of implementing a Biodiesel blend level sensor on a SOI platform. We show that dedicated waveguide configurations can be used for absorption measurements and we discuss the design of an integrated grating based SOI spectrometer with an on-chip sensing area for this application.

2. NEAR-INFRARED TRANSMISSION SPECTRUM OF BIODIESEL FUEL

We are interested in the region of high and measurable differences in the blends absorptions. Therefore the most promising regions to determine the blends are around 2100 nm, 1930nm and 1665nm. The transmission in the regions around 2100nm and 1930nm however is very low. The transmission in the 1665nm region on the other hand is higher and from this point of view, this region is more interesting. In the 1665nm region, a transmission difference of 20% is observed for the two fuel compounds, as is show below in Figure 1

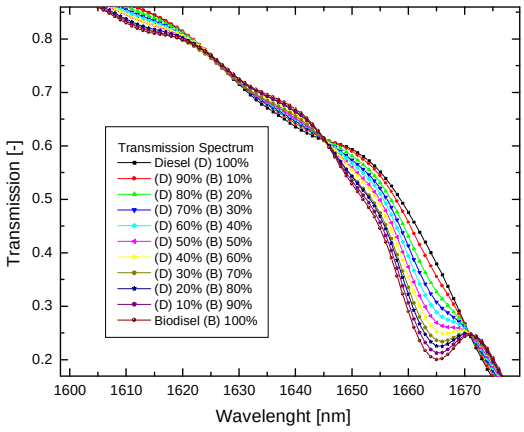

Fig 1.Transmission spectrum in percentage of different blends of Biodiesel in conventional Diesel fuel

3. DESIGN OF THE SOI CIRCUIT

The evanescent tail of the optical modes in the waveguides feels the fuel absorption processes. This interaction is proportional to the sensing length, and longer waveguides are necessary. These long lengths are achieved by curving the waveguide and creating a spiral shape waveguide. The interactions between the evanescent tail of the optical modes in the waveguides and the surrounding material are the key phenomenon in this sensing approach and we call them the sensing area in this work. We found optimum values of 1.1 and 0.22 cm for regular and slotted waveguides respectively . Fig 2. is a scheme for the designed spectrometer.

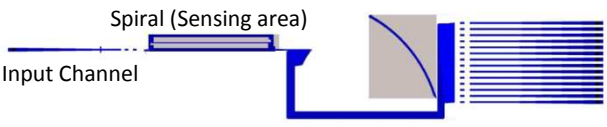

Fig 2. Scheme of planar concave demultiplexer, plus a spiral photonics wire.

4. SENSING BIODIESEL USING SOI STRUCTURES

For the first experiment, we fabricated spiral shaped 500nm wide photonic wire waveguides with different lengths. For these first experiments, the fuel was added manually on top of the sensing box.

The transmission spectra from the chip were measured with an Optical Spectrum Analyser (OSA) with resolution setting of 0.1nm. A superluminescence broadband Light Emitting Diode (SLED) with a center wavelength at 1650nm was used as the light source.

4.1 Sensing the Biodiesel blends.

A 1.1 and 3.6cm spiral were used as a sensing tool. Figure 3 compares the transmission spectrum measurement, for the predicted transmission values and the measurements for pure Diesel and pure Biodiesel. The measurements agree with our expectations and we found differences in transmission around 4dB at 1665nm, making possible the identification of the fuel composition.

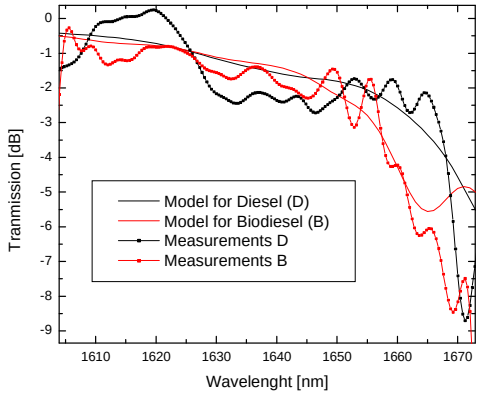

Fig 3. Transmission spectrum measurement, and model comparison for a 3.6cm spiral absorbing Diesel and Biodiesel

4.2 Sensing the Biodiesel blends using a 14 Channels PCG

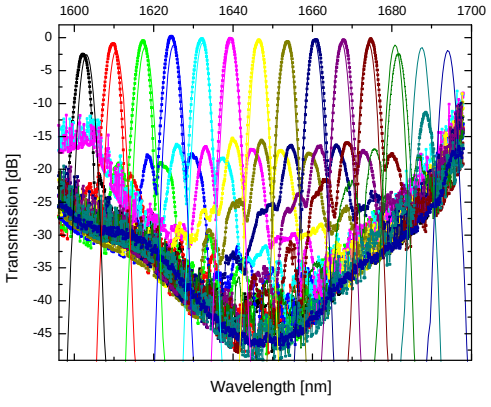

Fig. 4. Transmission spectrum measured for a 14 channel demultiplexer and simulation comparison

The 14 Channel PCG designed was characterized; First, we measure the transmission spectrum of a straight waveguide, and secondly we measure the transmission for each channel. These two transmission spectrums were normalized by subtracting both measurements. This was done for each of the 14 channels, thus, we obtain the 14 channel PCG characteristic spectrum which show us the total on-chip transmissions. The simulation performed is then compare with the measured values and are presented in Figure 4.

In concordance with our simulation we found 7 nm of channel spacing and a good response for almost all the channels. The measurements obtained show an improvement in the total on chip losses, and we obtain 0.46dB more than the simulated for the central channel. The crosstalk is better than 15dB.

By using a power meter we measured the power at the 8 central channels from our spectrometer-on-a-chip, thus we achieve the maximum absorption from the blends. In this experiment we add pure Diesel, pure Biodiesel and a 50/50 blend solution in to our sensing area.

Finally we compare the differences in transmission between pure Diesel and pure Biodiesel for the predicted and measured values, and we call these differences ΔFuel. We found correspondence for 6 of the 8 channels and they presented in Figure 5.

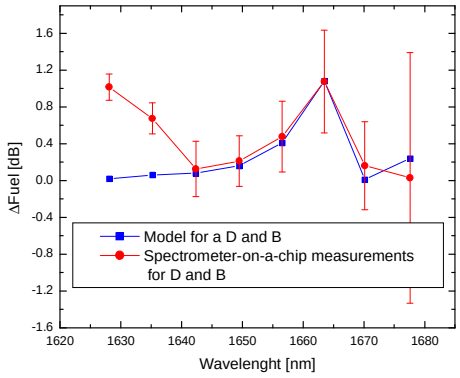

Fig. 5 Model and measured transmission spectrum differences between pure Diesel and pure Biodiesel for 8 different channels of our spectrometer-on-a-chip.

The long error bars in our measurements are caused due to the low power coming out form the corresponding channels. For the first two channels the measurements are not accurate most probably due to a low coupling efficiency caused by a shift in the input fiber in the cleaning process.

5. CONCLUSION

We have shown Silicon-on-insulator spiral shape waveguides are able to sense the absorption of Biodiesel/Diesel blends and can incorporate these spirals successfully with the planar concave demultiplexer. Thus, the PCG and the spirals fabricated act as spectrometer-on-a-chips, sensing the blends at different wavelengths.

Using the fabricated spectrometer-on-a-chip with the 1.1cm spiral, we measured the transmission spectrum for pure Diesel, Biodiesel and a 50/50 blend. For a particular point in the high absorbing region, (1663.48nm), we predicted 1.08 dB and we measured 1.075 ± 0.559dB for the difference Biodiesel-Diesel, and for the 50/50 blend, we predicted 0.56dB and we measured 0.339 ± 0.509dB for the difference Biodiesel-50/50 blend.

Content

List of Figures

Abbreviations and Acronyms

Biodiesel (B)

Benzocyclobutene (BCB)

Carbon Dioxide (CO_2)

CAvity Modelling FRamework (CAMFR)

Complementary metal–oxide–semiconductor (CMOS)

Diesel (D)

Distributed Bragg Reflectors (DBR)

Graphic Data System (GDS)

Inductive Coupled Plasma (ICP)

Metal-Semiconductor-Metal (MSM)

Multivariate analysis (MVA)

Near Infrared (NIR)

Planar concave grating (PCG)

Reactive Ion Etching (RIE)

Scanning Electron Microscopy (SEM)

Silicon-on insulator (SOI)

Spectrum Analyzer (OSA)

Superluminescence Broadband Light Emitting Diode (SLED)

Transverse Electric mode (TE)

Transverse Magnetic mode (TM)

Ultra Violet (UV)

1. Introduction

Biodiesel is a biofuel with methyl esters as a primary compound. These can be produced from different types of biomass, including animal fats, waste cooking oil and oilseed rape. Oilseed rape, in particular, is one of the principal sources of biofuel because it can be cultivated on a fairly wide range of agricultural land. Biofuel has become potentially important because it is a nontoxic, biodegradable and renewable source of energy that, in contrast to conventional Diesel fuel [(2)], reduces the carbon dioxide (CO_2) emission in a combustion process. Therefore, the emission of greenhouse gases which are in big part responsible for the climate changes is also reduced.

Biodiesel can be used in Diesel engines as a pure fuel or in blends with Diesel fuel. To maintain optimum performance and meet emission regulations, it may be necessary to measure the composition of blended fuels and adjust engine parameters such as fuel injections timing during operation. [(2)]

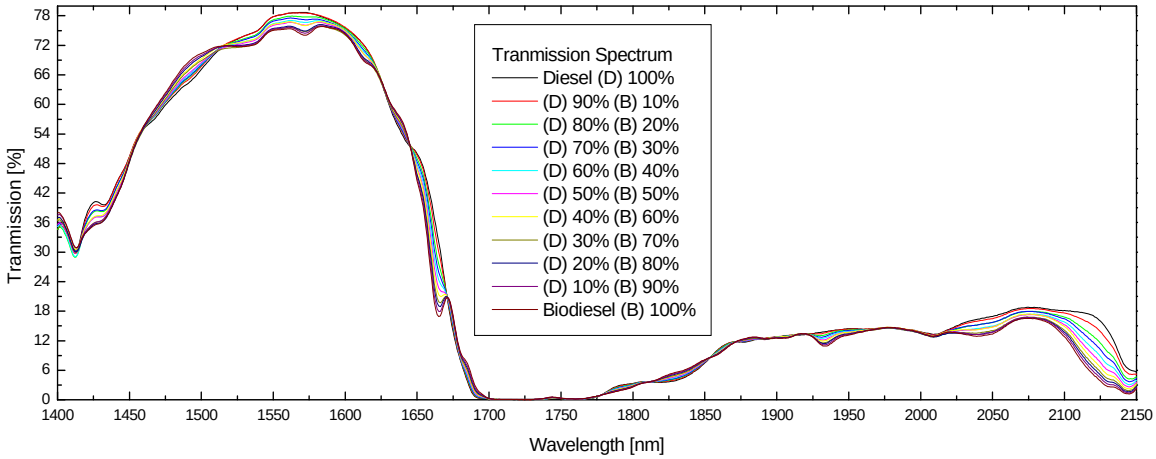

Figure 1 - 1 Percentages of transmission for different blends of Biodiesel and conventional Diesel fuel with an optical path length of 1cm[(3)]

Previous studies [4; 5; 6] have showed that near- and far-infrared absorption spectroscopic techniques are good tools to determine the Biodiesel/Diesel blend levels. By measuring the absorbance of the mixture in these wavelength ranges, it is possible to predict the blend level with good accuracy, as is shown in as is shown in (Figure 1 - 1). This figure plots the transmission through a 1 centimeter cuvette filled with a mixture of Biodiesel/Diesel as a function of wavelength.

Conventional photospectrometers are typically large and expensive and have a performance that often exceeds the requirements for most applications. For automotive applications for example, what counts is size, robustness and most importantly, cost. As a result the miniaturization of the spectrometer can be seen as an attractive Biodiesel sensor implementation, which can be used to adjust fuel injection timing during operation. A planar concave grating (PCG) is an interesting wavelength filter for spectrometer applications due to its possible small size, high resolution and large channel count. PCGs have been realized in many material systems including silica-on-silicon, III–V's, large core silicon-on-insulator (SOI) substrates [7] and nanophotonic SOI substrates [8; 9]. The SOI platform, particularly, is a promising material system for a wide range of applications, such as telecommunications and optical sensors. Due to the large omnidirectional index contrast of this material system, these devices can be made very compact and they can be manufactured on high-quality SOI substrates using CMOS fabrication tools, making these devices cheap for the market.

1.1. Aim of the Project

The final goal of this project is to fabricate a photonic integrated chip able to sense Biodiesel/Diesel blends using a Near Infrared (NIR) absorption spectroscopy. This system is based on Planar Concave Grating demultiplexer on a Silicon-on-Insulator. The proposed chip design consists of a fiber coupler, a PCG, a sensing SOI platform and InGaAs metal-semiconductor-metal (MSM) photodetectors heterogeneously integrated on top of the outgoing SOI waveguides.

The schematic presented in Figure 1 - 2 is a view of the spectrometer-on-a-chip design. Light is first coupled from fiber to the chip via planar grating couplers. A Input single mode fibers is aligned and glued on top of the fiber couple under a 10 degree angle from verticality using an UV-curable glue.

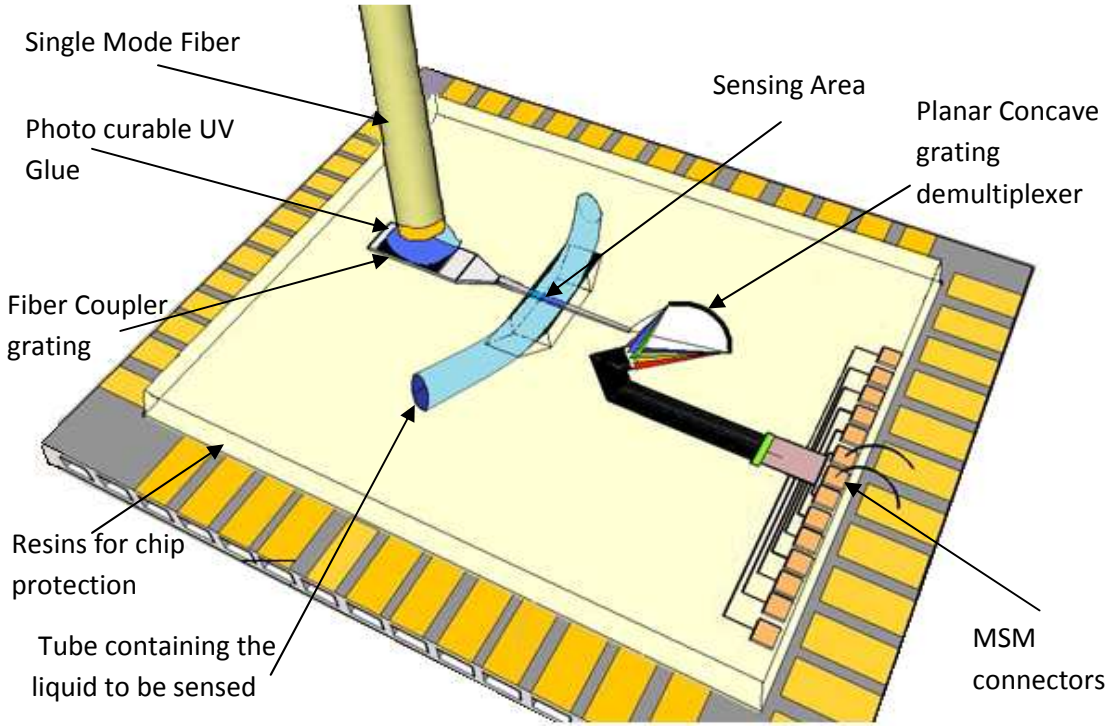

Figure 1 - 2. Schematic view of spectrometer on a chip adapted for a Fuel sensing application

The light is guided trough the photonic wire and crosses the area designed specifically to feel the absorption processes. Next, the light is guided to the PCG demultiplexer which separates and focuses the light into 14 different wavelength channels. 14 InGaAs MSM photodetectors are to be integrated on top of the 14 output waveguides to measure the optical power in the 14 different wavelength channels and to obtain the absorption values at the corresponding wavelengths.

In this work, we did not integrate MSM photodetectors but their functionality [10] and the heterogeneous integration with a PCG has been successfully studied previously [3].

In the subsequently pages we demonstrate the feasibility of implementing a Biodiesel blend level sensor on an SOI platform. We show that dedicated waveguide configurations can be used for absorption measurements and we discuss the design of an integrated grating based SOI spectrometer with an on-chip sensing area for this application.

The document is organized as follows: In Chapter II, we discuss the Near infrared spectroscopy, the transmission spectra for different Biodiesel/Diesel mixtures in the near-

infrared wavelength range, the theory, design and optimization for Silicon-on-Insulators, Planar concave Gratings and sensing arquitectures. We explain in chapter III the fabrication steps used during this work. We discuss the fuel measurement results in chapter IV and we conclude in chapter V.

2. Near Infrared (NIR) integrated absorption spectroscopy with SOI structures

The design and optimization of the constituent elements of the integrated infrared SOI based biodiesel sensor are the major issues discussed in this chapter. Here we introduce the concepts behind the NIR spectroscopy, we show and discuss the NIR Biodiesel/Diesel blends absorption spectrum, we explain briefly the principles of the SOI structures, how they can be designed as a demultiplexer tool, and how the integration of photonics wires with a demultiplexer can function as a sensing tool for the Biodiesel. Finally, we estimate the expected Biodiesel sensitivity of our device using simulation tools as Fimmwave [(11)] and CAvity Modelling FRamework (CAMFR) [(12)]. These results are to be compared with the absorptions measurements in chapter 4.

2.1 Near infrared absorption spectroscopy.

Near infrared (NIR) spectroscopy uses light in near infrared region, 780nm to 2500nm to measure the matter absorption. When the light radiates on the sample, the sample absorb, scatters or transmits the light, these interaction can be measured by knowing the light properties before and after penetrating through the sample.

If the energy or frequency of an incoming IR photon matches the energy needed to excite the atom-to-atom bonds contained in a sample, the IR photon will be absorbed by the molecules, and the molecules will be excited to higher energy state. This absorbed energy will be reflected in the transmission spectrum, leading to a low transmission point, and therefore the fingerprint or characteristic molecule interaction can be recognized form this process.

Different molecules have different bonding strength and hence different vibrational frequencies. This renders each molecule a unique body with different identification. Therefore, near infrared spectroscopy is popular for qualitative analysis and quantitative measurements of functional groups of OH, CH, NH and CO and has been widely adapted as a sensor in many industrial applications, i.e. pharmaceutical, food and beverages.

For biodiesel for example the primarily compound are the methyl esters, which are formed basically[2] by the chain 3R-$COOCH_3$. Here, R is mixed fatty acid of linseed oil. The bond between these chains are then present in the NIR region, and for that reason, is easy to study its composition by using NIR spectroscopy.

2.1.1 The Beer Lambert Law & the NIR region for sensing

Using a logarithmic scale, Beer Lambert shows the relationship between the light power before (P_1) and after (P_0) passing a sample. These two magnitudes are connected logarithmically with the absorbance (A) for a particular wavelength as is expressed in Equation (2-1)

$$\boldsymbol{A = -Log_{10}\left(\frac{P_1}{P_0}\right)} \qquad \textbf{(2- 1)}$$

Here A is the product of the absorption coefficient (α) by distance the light travels through the material (i.e. the path length), ℓ.

The link between NIR infrared spectroscopy and the Beer Lambert law is based on the accessibility of the frequencies resonances for the particulars bonds in the infrared region. For that reason by combing the Beer Lambert law and NIR spectroscopy it is possible to obtain the absorption characteristics from a particular material, which in our case is Biodiesel/Diesel blends.

2.1.2 Near- infrared transmission spectra of Biodiesel fuels

Using infrared spectroscopy the blend level of the Biodiesel/Diesel mixture can be analyzed. In a previous work [3] different samples with different blend levels were prepared and characterized. The transmission spectra of the samples were recorded with a CARY 5000 UV-VIS-NIR photospectrometer by Varian. For these measurements, they used a plastic

cuvette with an optical path length of 1cm containing the Biodiesel/Diesel mixtures. Using the Cary WinUV software, the recorded transmission spectra were taken in the wavelength range of 1400nm to 2400nm, with a resolution of 1nm, as was presented in Figure 1 - 1.

We are interested in the region of high and measurable differences in the blends absorptions. Therefore the most promising regions to determine the blends are around 2100 nm, 1930nm and 1665nm. The absorption in the regions around 2100nm and 1930nm however is very low. The absorption in the 1665nm region on the other hand is higher and from this point of view, this region is more interesting. In the 1665nm region, an absorption difference of 20% is observed for the two fuel compounds, as is show below in Figure 2 - 1.

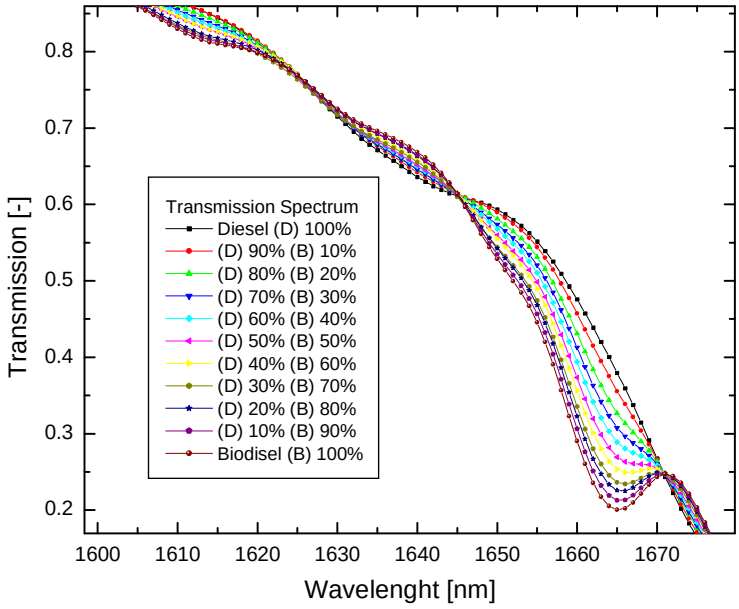

Figure 2 - 1. Transmission spectrum in percentage of different blends of Biodiesel in conventional Diesel fuel

To define the number of wavelength channels of the planar concave grating demultiplexer a better spectral localization of these differences is needed. This localization can be done by taking the second derivative of the transmission spectrum in the 1665nm region, (Figure 2 - 2). As can be seen, ten peaks at different wavelengths in the 1600-1700nm region are identified.

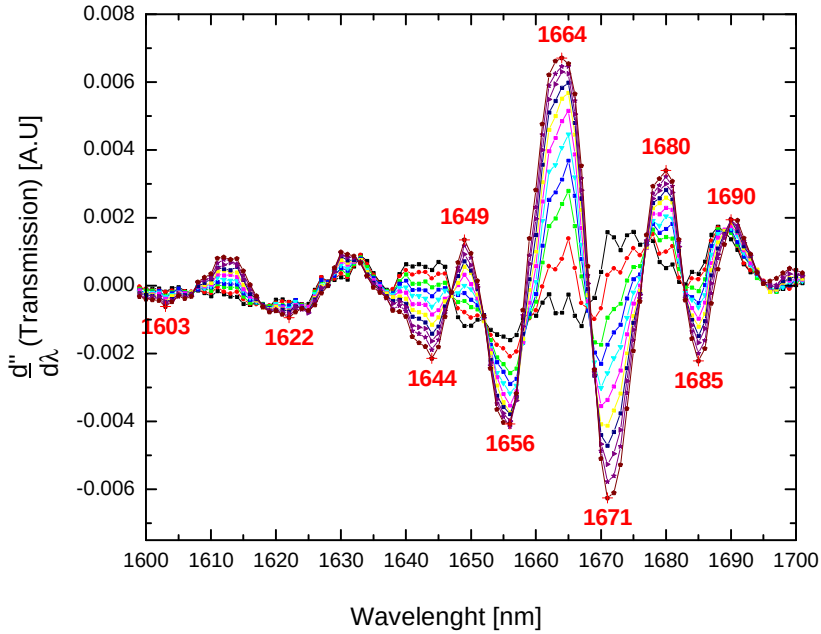

Figure 2 - 2. Second derivative of the transmission spectrum around 1665nm

Each of these differences are spaced by 7 nm. The identification of these peaks helps us to design the number of exit channels in our demultiplexer and in addition, by using a statistical technique called Multivariate analysis [3], the observation and analysis of more than one statistical variable at a time can be used to predict the concentration or blend constitution.

2.2 SOI based integrated biodiesel sensor

High refractive index contrasts brings control over a wider range of propagation directions, moreover the propagation angles are larger, and thus the structures can be bended over a few micrometers. In this work we use a SOI material stack with a 220nm thick crystalline Si core layer separated from the Si substrate by 2 µm thick amorphous SiO_2 bottom cladding, the top cladding in our case is air or fuel to be sensed, this waveguide geometry is illustrated in Figure 2 - 3, and the refractive indices for these materials are presented in Table 1

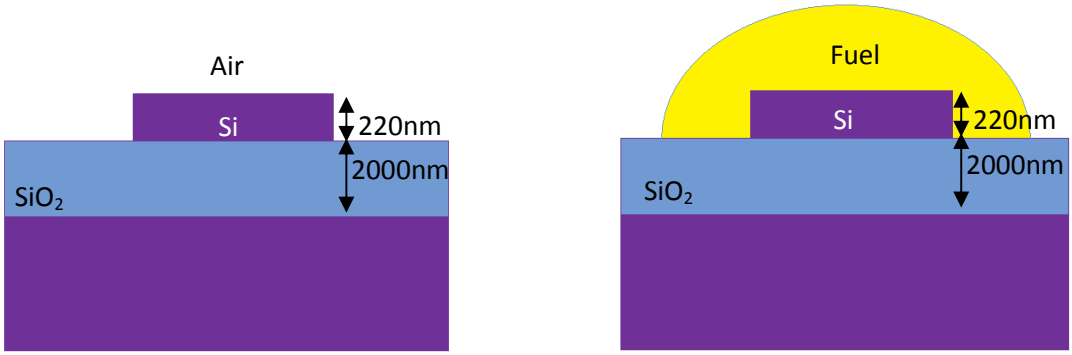

Figure 2 - 3. Cross section view of the silicon-on-insulator wires used throughout this work

	cSi	SiO_2	Biodiesel
n	3.469	1.442	1.455[6]

Table 1. Refractive indexes of crystalline Si (cSi), amorphous SiO_2, and Biodiesel, at 1650nm wavelength and 300K.

It is possible to fabricate single-mode propagation submicron photonic wire by using SOI structures. The small dimensions of these arquitectures requires a nanometer-precision fabrication and in this work we have used deep 193nm deep UV lithography.

SOI structures are totally convenient for integrated arquitectures, because using CMOS technologies different arrays can be done and the light can propagate and interact with these structures very efficiently. But is the evanescent tail of the optical modes outside the Si the principal phenomena in this integrated Biodiesel detector.

2.2.1 Confinement factor

Most of the light propagates inside the waveguide core due to the high refractive contrast achieved by the SOI structures, but here, it is the evanescent tail of the optical modes outside the Si waveguides that feels the fuel absorption processes.

This Biodiesel/Diesel blends absorption from the different waveguide configurations can be described using the Beer-Lambert law. Taking into account the absorption of the material, and the interaction distance *x*, we create a model for a sensing area:

$$P_1 = P_0 . 10^{-\Gamma . \alpha . x} \quad \textbf{(2- 2)}$$

Here Γ is the confinement factor[1], P_0, and P_1, are the input and exit powers and α is the absorption coefficient of the surrounding material. The confinement factor is a good measure for the amount of light that interacts with the surrounding fuel. This value is the fraction of the intensity in the fuel region over the total intensity.

The intensity profile of the propagating electric field is simulated for slotted and regular waveguides. These calculations were made using Fimmwave [(11)], a fully vectorial mode solver. The intensity color map in Figure 2 - 4 shows how the TE_{00} propagating mode is confined mostly in the core of the waveguide, however a large part of the electric field is also present in the cladding and in the free region; this last one, is where the evanescent tail of the optical mode feels the fuel absorption processes.

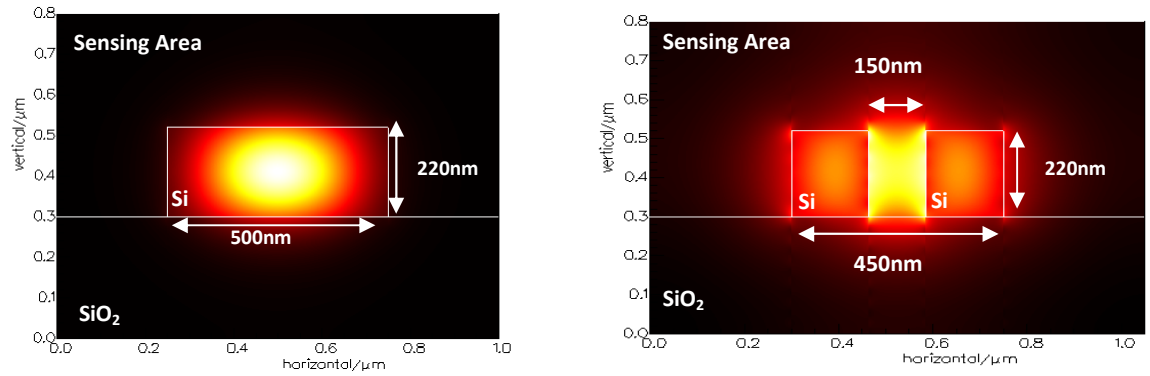

(a) (b)

Figure 2 - 4.Fimmwave simulation for the intensity profile of the fundamental TE-polarized mode in a Regular (a), and Slotted (b) waveguide. Using $n_{Biodiesel}$ = 1.455; n_{Si}=3.466; n_{SiO2} =1.442, refractive indices.

Fimmwave solves the Maxwell equations and gives solutions in 2D from confinement factor in the region of interest, we performed simulation changing different parameter as the width and the depth for slotted and regular waveguides. Figure 2 - 5 shows the results of the confinement factors of both waveguides. The maximum confinement factor is 77% for a slotted and 21% for a regular waveguide.

[1] The confinement factor is defined as: $\int_d^{\infty} E^2(x,y)dxdy / \int_{-\infty}^{\infty} E^2(x,y)dxdy$, where d is the slab thickness.

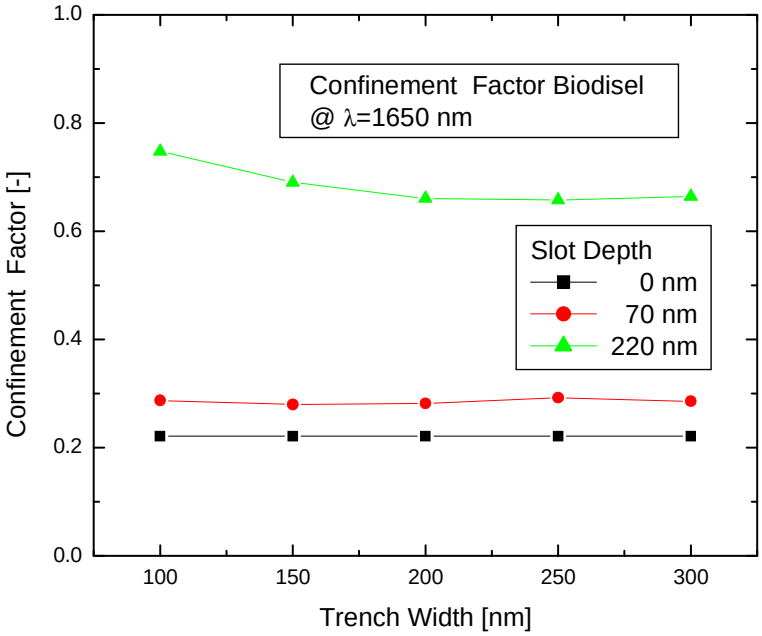

Figure 2 - 5. Simulation results of the confinement factor of slotted and regular waveguides. The slot depth varies from 0 to 220 nm high. The width from 100 to 300nm

By knowing the modal overlap between the Biodiesels/ Diesel blends and the propagating light, we can predict how much of the light will be absorbed by the fuel and thus its constitution.

2.2.2 Sources of loss

Propagation losses in straight SOI wires arise from different sources, these includes Bulk and non linear absorptions, substrate leakage, and Rayleigh and sidewall roughness scattering[13]. The Bulk Si has a negligibly low absorption $\left(0.02\frac{dB}{cm}\right)$ around 1650nm. The nonlinear absorption arise from high power interaction, the power used during this work does not exceed the 12 mW, therefore nonlinear effect are not considered, equally for the Rayleigh scattering, where the λ^4 effect is totally minimized due to the high crystalline semiconductor material used as a core.

Light is scattered at irregularities, both on the sidewalls and top and bottom walls of the core, these are the major cause of propagation losses and are reported for the TE_{00} around 0.1 $\frac{\frac{dB}{cm}}{nm^2}$. The silicon also has some roughens primarily from polishing process, therefore another

source of scattering losses are incorporated. The scattering losses become important and are minimized when the refractive index of the top cladding decrease the refractive index contrast with the core. We will show in the next chapters that these losses are present in our measurements and become visible at the moment of getting conclusions.

The coupling efficiency from fiber to chip is also crucial in our design. We want to couple the biggest amount of light in to chip and also recover the information after the light has moved around our device. Previous research [14] has shown an efficient way to couple light from the fiber into the chip and vice versa, by using grating couplers, no lenses or focusing gratings are needed, and indeed 38% of coupling efficiency can be achieved.

The high refractive indexes contrast of the nanophotonics wires makes them polarization sensitive, where the boundary conditions at the steps are different and as a result the propagation constant of the TE and TM modes are also very different. The grating couplers designs are also optimized for the TE propagation mode, and for that reason we incorporate this grating in our work. A draw of this vertical coupler is presented in Figure 2 - 6.

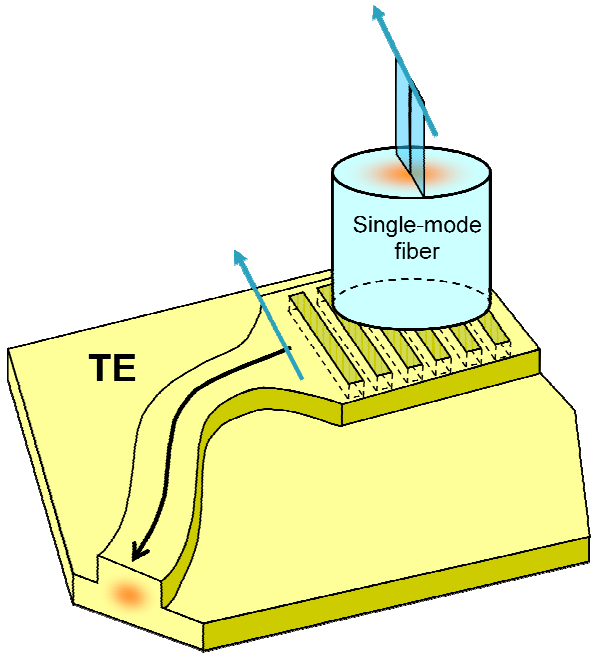

Figure 2 - 6. Schematic vertical coupler used to couple light from the fiber into the SOI structure and viceversa [14].

Finally the substrate leakage losses are considered in this work the most important ones, because these losses interact with the material to be sensed, in other word the tail of the

modes which is exponentially decreasing outside the core is coupled in the Biodiesel/Diesel blends and thus the absorption take place for the different wavelengths.

We designed a platform using Mathematica[15] able to solve the 1D Maxwell equation for a propagating TE_{00} mode inside a rectangular waveguide, the parameters imposed to this design are presented in Table 2, and the solution for the intensity profile is plotted and presented Figure 2 - 7.

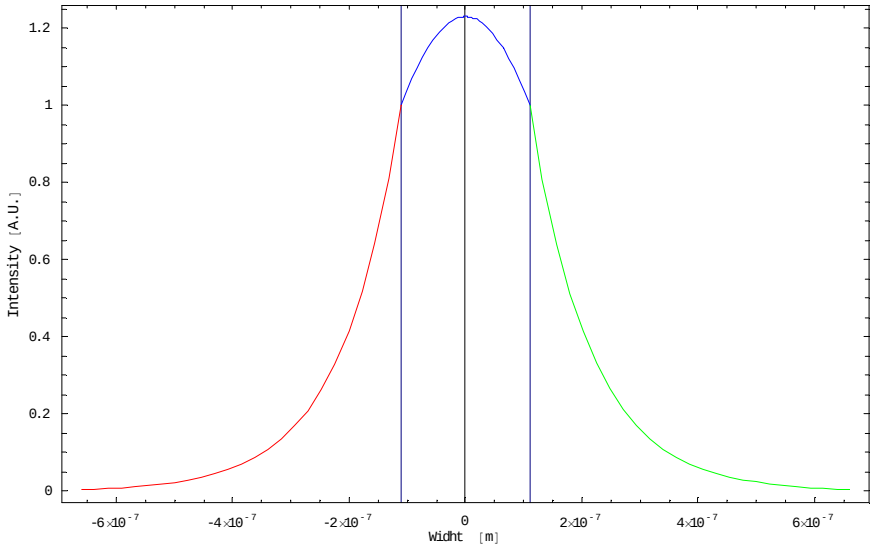

Figure 2 - 7. Mathematica Simulation made for a TE_{00} mode Intensity profile propagating inside a rectangular box, The green line is the evanescent intensity tail which is contact with the Biodiesel/Diesel Blends.

Propagating wavelength	1650 nm
Slab thickness (d)	220 nm
Biodiesel Refractive index n_3	1.455
Si refractive index n_2	3.476
SiO_2 Refractive index n_1	1.442

Table 2. Parameter used for the Mathematica simulation platform.

On the other hand as a first approximation, this platform helps us to obtain values as confinement factor and good 2D and 3D visualization. Below in Figure 2 - 8 we present a 3D solution for the propagating intensity field in a SOI configuration with a given refractive indexes of (1.755) on top of Si and (0.442) for the cladding

The confinement factor value obtained using these set of arbitraries refractive indexes was 29.616 %, but using the parameter described in Table 2 we obtain a confined factor of 22.589 %, 1% higher than the value obtained in section 2.2.1. Caused because our model

does not consider the width of the SOI, only consider the height of Si core and also because we have used a particular solution for solving the Maxwell equation, while Fimmwave do the same calculation in a rigorous way.

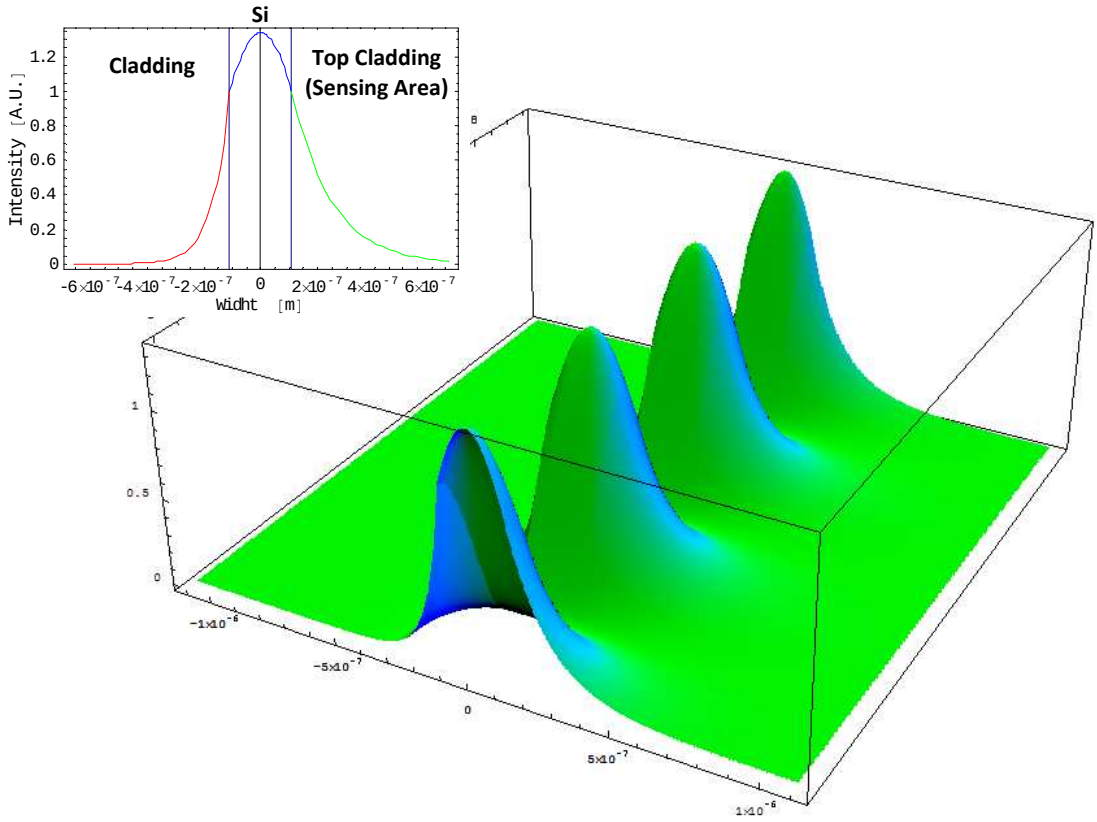

Figure 2 - 8. 2D and 3D Simulation for a propagating Intensity field in a SOI structure with a given refractive index of (1.755) on top of Si, and given refractive index (0.442) for the cladding.

The platform is described in detail in the Mathematica file and can be found in the appendices 6.1 of this document, we also compare our results using Fimmwave, and a contour plot in 2D was produced for the same waveguide parameters from Table 2 as is seen in Figure 2 - 9. We found correlation for the visualization with our platform.

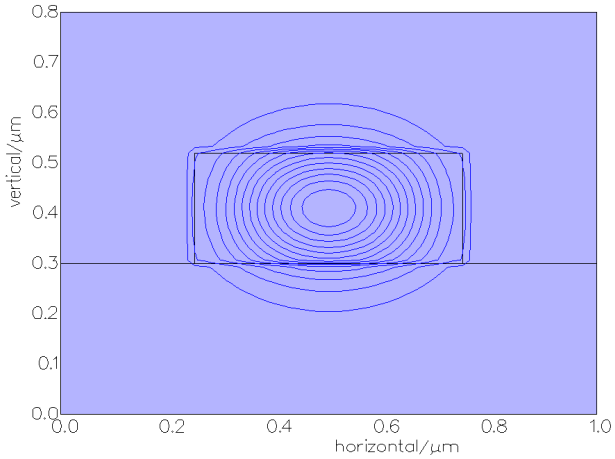

Figure 2 - 9. Intensity contour plot simulation for a TE_{00} in a rectangular waveguide

2.2.3 The Planar Concave grating demultiplexer (PCG) plus distributed Bragg reflectors (DBR)

Configurations as a planar concave demultiplexer can be realized with SOI technologies, and the principal advantage that overcomes, is the miniaturization of this structure which works as spectrometer, in this section we are going to explain how a PCG works and how we changed the design parameters to fulfill the requirements of our biodiesel sensor.

The light is traveling inside the Si core, here it can take different direction or paths depending of the arrays created, therefore by implementing a grating element it is possible to diffract the light and give the direction that we decide.

The PCG uses the Rowland circle theory, this configuration is well-know, and widely described in literature [16]. Its working principle is based on its diffraction grating which is the responsible for splitting the light and diffracting it in several beams traveling in different directions. These directions depend on the spacing of the grating facets and the wavelength. The input and output waveguides are positioned along a circle with radius *R* called the Rowland circle, the grating facets sit on a grating circle with radius *2R* and both circles touch at the middle of the grating as is presented in Figure 2 - 10.

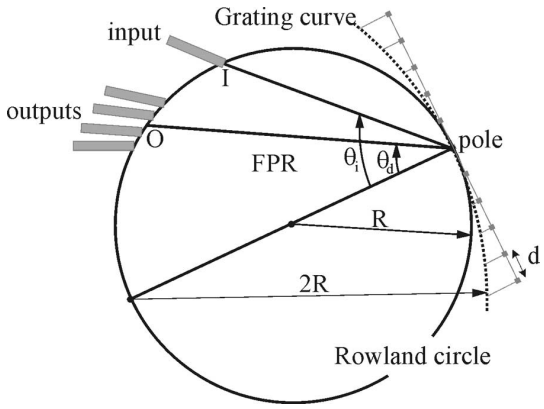

Figure 2 - 10. PCG demultiplexer based on Rowland configuration.

All the waveguides incorporated in this device ends in an unetched slab region, the lights that come out from the input waveguide is expanded in the free propagation region and travel into the direction of the grating, this concave grating act as a mirror diffracting and focusing the diffracted light into a series of output waveguides positioned on the Rowland circle. The grating equation is given by:

$$\boldsymbol{d(\sin\vartheta_i - \sin\vartheta_d) = m\frac{\lambda}{n_{eff}}} \qquad \textbf{(2- 3)}.$$

This relationship relates the grating period (d), the incident (ϑ_i) and diffracted (ϑ_d) angles, with the order of diffraction *(m),* the wavelength (λ) in the vacuum and the effective index (n_{eff}) of the slab mode. In this way the condition for constructive interference and the fact the light with the same wavelength is focused in the same point, is explained.

By designing a PCG with 14 output channels with a channel spacing of 7nm, each of the peaks found in Figure 2 - 2 are reached, therefore to measure the transmission at the different wavelengths of interest we have designed a 14 channel PCG and incorporated DBR grating facets. In our design, the DBRs have four periods. Figure 2 - 11 is a schematic view of the PCG and part of the DBR grating.

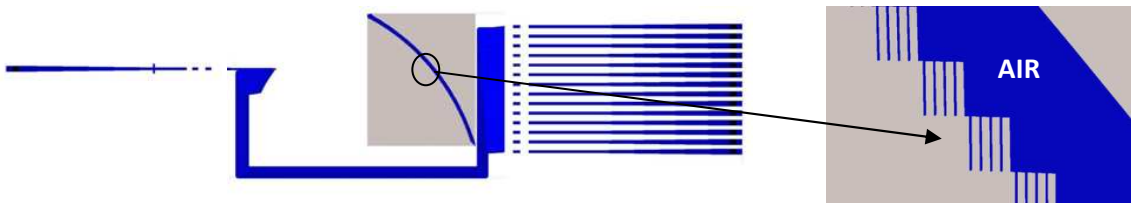

Figure 2 - 11. Schematic for a 1x14 PCG demultiplexer designed in this work and DBRs added to grating.

The dimension implemented in our design has a grating period *d* = 4.7258µm, Rowland radius *R* = 561.912µm, input angle ϑ_i = 41°, first diffracted angle ϑ_d = 37°, order of diffraction *m* = 10, a calculated effective index n_{eff}=2.7756, 91 facets and 5 µm of spacing between the 14 output channels.

We first simulated the Transmission spectrum of the PCG, changing the number of reflecting facets (Figure 2 - 12), and we found an exponential decay, that after 80 facets take a constant value around 0.5dB, therefore considering this behavior, we took 91 facets for the grating in our design.

The simulated transmission spectrum of a demultiplexer is presented in Figure 2 - 13. One input waveguide and 14 output waveguides are considered in these simulations. The channel spacing is 7 nm. The size of the diffraction grating, with the 91 facets, is about 440µm.

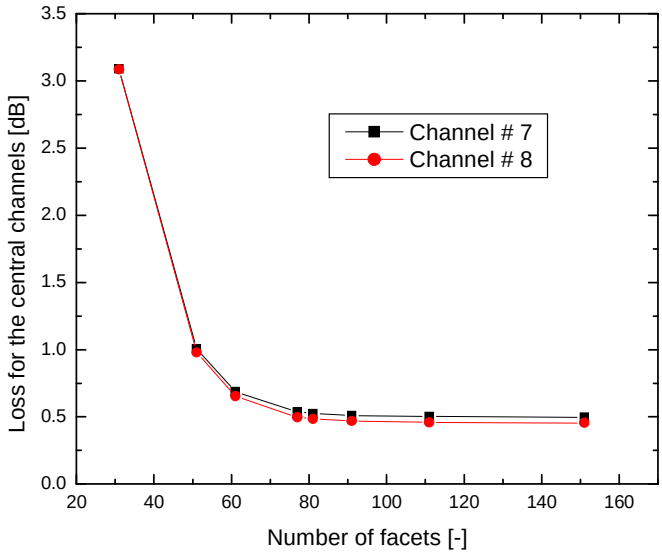

Figure 2 - 12, Minimum transmission spectrum point for the two central PCG channels versus number of facets

The simulation of the PCG spectrum is done using scalar diffraction theory (Figure 2 - 13). For these simulations, we take into account a perfectly reflecting grating (R=1). This means these results give information on diffraction losses, crosstalk, channel spacing and loss variation over the total wavelength range. This design has a diffraction loss of about 0.5 dB for the central channel (1650nm), and 30dB crosstalk.

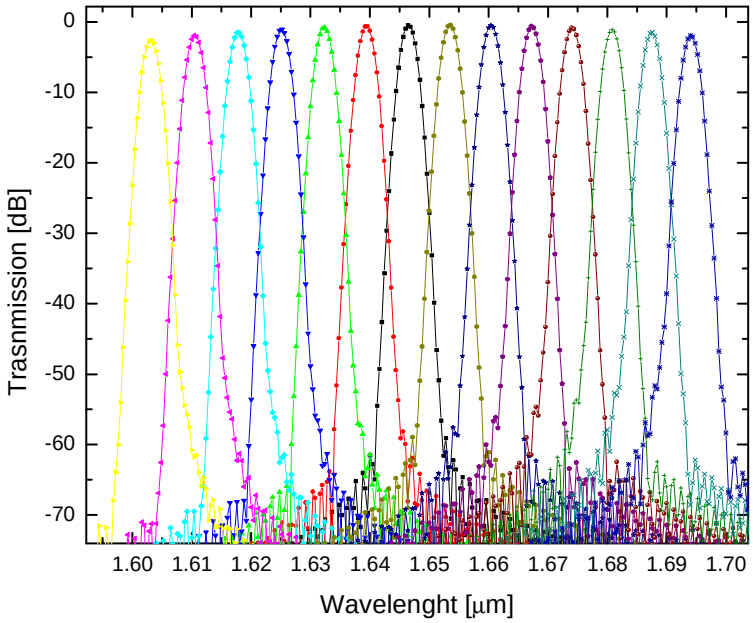

Figure 2 - 13. Simulated transmission spectrum for 14 channels demultiplexer

The grating facets are acting as a mirror and are the responsible for the diffraction. In previous publication [17; 18] has been shown that using a second order DBRs the reflection losses can be improved and decreased from 4.9dB down to 1.0dB, as we will show in chapter 4, for the measurements.

The basic working principle behind this effect is the Bragg condition, which for Si and Air, can be expressed as:

$$\boldsymbol{n_{Si}.h_{Si} + n_{Air}.h_{Air} = m\frac{\lambda}{2}} \qquad \textbf{(2- 4)}$$

Here (*h)* is the width of the material and (*n)* is its refractive index, the reflected constructive interference can then achieved by the correct array of this magnitudes.

In our design we include a deeply etched (220 nm) second-order DBR consisting of four periods with 145nm width for air (etched part) and 524.2nm width for Si. To calculate the total on-chip loss of the PCG, we also need to take into account the grating reflection loss. The reflection of the DBR facets is calculated using CAMFR. The results from this simulation are presented in Figure 2 - 14 as can be seen, the reflection at the central wavelength is 89%. This corresponds with a grating reflection loss of 0.5dB.

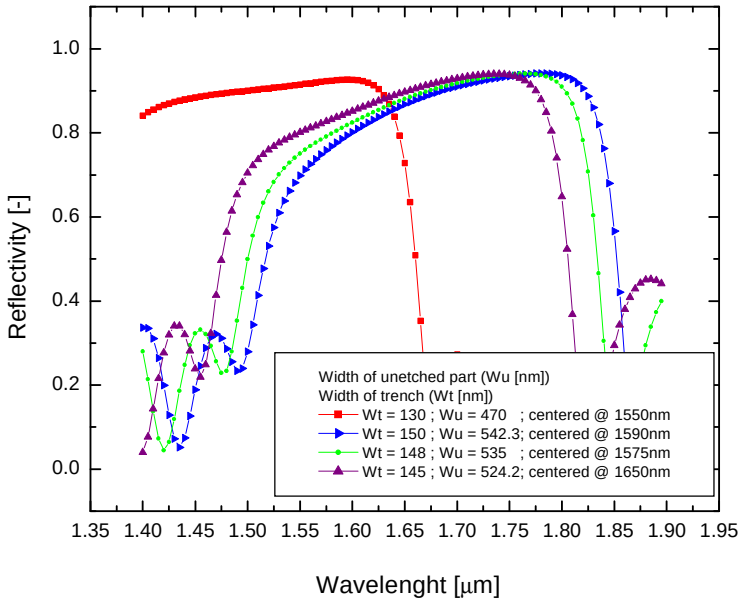

Figure 2 - 14. Simulation results of the reflectivity of a four-period DBR-type facet. The period is 670 nm and the trench width varies from 130 to 150 nm, the unetched part from 470 to 542.3 nm. Perfect vertical sidewalls are supposed

The coupling efficiency was also calculated using CAMFR, the parameter analyzed were the input angles and the grating period. (Figure 2 - 15). Here at 10 degrees angle we found the optimal position for the wavelength of interest 1650nm, achieving 4.87 dB of coupling efficiency, and the grating period for the couplers was 680nm.

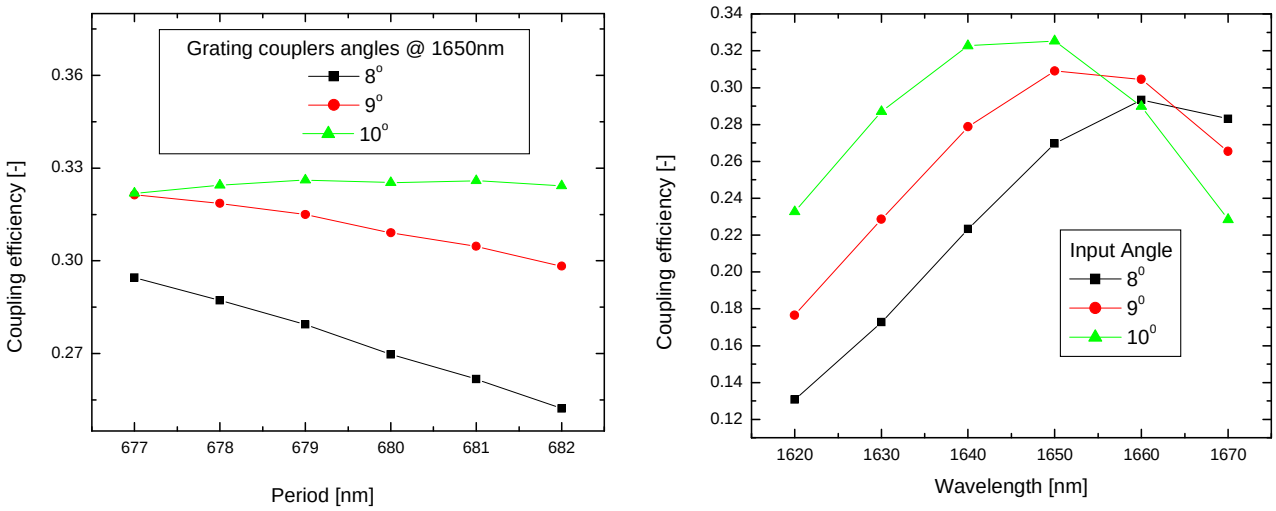

Figure 2 - 15. Simulation results of coupling efficiency by changing the optic fiber input angle and the grating period

2.2.4 The spiral waveguides and sensing area

The evanescent tail of the optical modes in the waveguides feels the fuel absorption processes. This interaction is proportional to the sensing length, and thus, longer waveguides are necessary. These long lengths are achieved by curving the waveguide and creating a spiral shape waveguide. The interactions between the evanescent tail of the optical modes in the waveguides and the surrounding material are the key phenomenon in this sensing approach.

Figure 2 - 16, presents a spiral photonic wire photograph, which was took by using a Scanning Electron Microscopy (SEM). This spiral has 11394mm long, 500nm width, 20nm of radius and 6 loops.

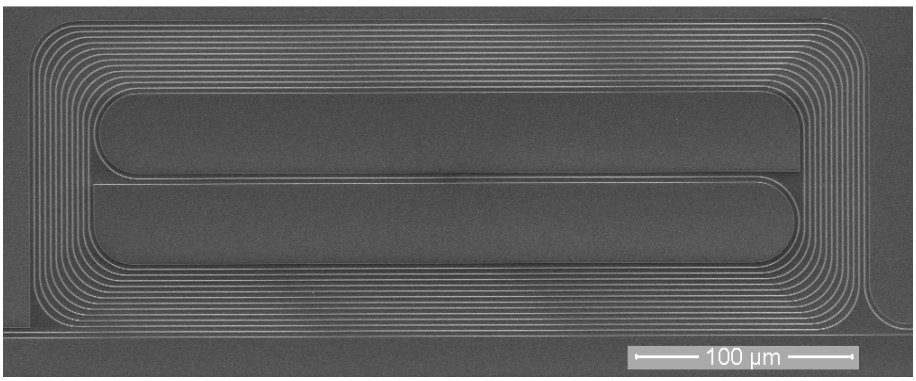

Figure 2 - 16. SEM photograph of a Spiral photonic wire. [19]

It is also possible to obtain the absorption information using structures which have a higher interaction with the surrounding material; this is the case for slotted waveguides. These waveguides are fabricated by etching a very narrow slot in the middle of a conventional waveguide. The intensity in the slotted area is very high [20] and, an intensity plot for a slotted waveguide was presented previously in Figure 2 - 4(b).

The Biodiesel/Diesel absorption occurs in these waveguide configurations, and we have called them the sensing area in this work.

2.2.5 Integrated detectors

For the goal of this project the inclusion of integrated photodetectors by heteroepitaxial growth of III–V materials, is the most feasible solution [10; 21], these detectors are formed by layers of Metal-Semiconductor-Metal (MSM).

The semiconductor InGaAs is a highly absorbing material in the near infrared region and is commonly used for the fabrication of NIR photodetectors. We present in Figure 2 - 17 a schematic three-dimensional (a) and cross-sectional (b) views of waveguide integrated MSM detectors.

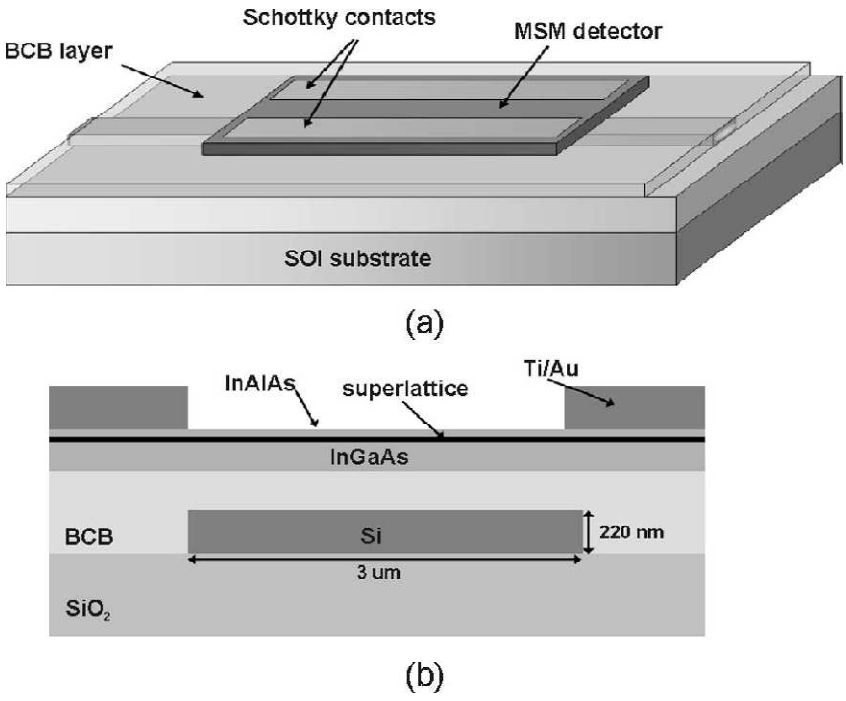

Figure 2 - 17. (a) Three-dimensional and (b) cross-sectional views of waveguide integrated MSM detector [10].

The III-V material can be heterogeneously integrated on the SOI substrate using adhesive bonding by means of BCB as an intermediate bonding layer, this way the photodetectors can be lithographically aligned onto the SOI waveguides

A previous research [3] developed a complete set of integrated photodetectors (Figure 2 - 18) for a 1x30 PCG demultiplexer, showing a solution of integration and possible implementation for the goal of this project.

Figure 2 - 18. Photograph for the complete set of 30 III-V photodetectors bonded on SOI waveguide circuit[3]

For time reason's we did not integrate MSM photodetectors in this work, but their functionality [10] and the heterogeneous integration with a PCG has been successfully studied previously [3]. However as an immediately solution, we used a power meter for measuring the exit power from the 14 channels.

2.3 Modeling the absorption for the Biodiesel/Diesel blends using a spiral shaped waveguide.

The interaction length between the Spiral and the Fuel is called the sensing area in this work. By using the simulations software's and Equation (2-2) we create a model able to predict the fuel transmission spectrum using a spiral photonics wire structure.

The model uses the fuel absorptions obtained from the spectrum in Figure 1 - 1, the confinement factor obtained from the simulations, and the propagation losses from the regular spiral shaped waveguides. We show the predicted values in Figure 2 - 19.

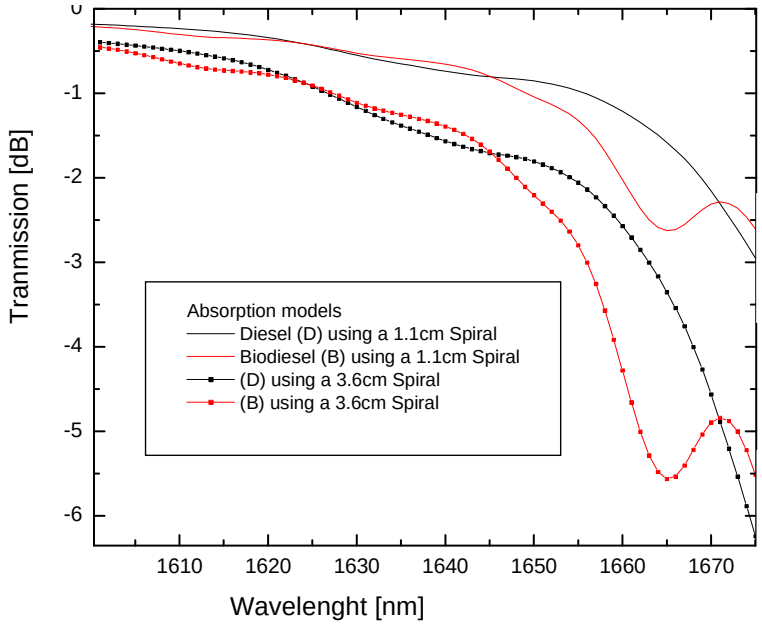

Figure 2 - 19 Model for the Biodiesel/Diesel transmission spectrum for a 1.1 and 3.6 cm long spirals

This model shows the fuel transmission spectrum obtained by using 1.1 and 3.6 cm spirals photonics wire measured by a conventional spectrometer. Here we observe for higher wavelengths more absorption i.e. less transmission. The model also predicts higher absorption for the longest spiral which in our case has 3.6 cm long, moreover the difference between pure Diesel and pure Biodiesel also increase.

2.4 SOI spectrometer-on-a-chip design implemented in this work

The final design implemented for our spectrometer-on-a-chip was made by considering all the simulations, losses and predictions mentioned previously. Our goal is to obtain the maximum absorption from the fuel, but also be able to detect it.

We know that the differences in transmission are larger for longer waveguides, but all the measurements are also limited by different factors. These factors are: The power for the source, the coupling efficiencies, the losses on the chip and the power at the exit channels, moreover this last one should be large enough to be detected. Consequently the sensing area and its length are also limited by these values. These parameters are already considered and the design is optimized. To find this length, we obtained that the fiber coupling losses are (2 x 4.877 dB). For the central channel at the PCG the diffraction loss and the DBR loss are 0.5dB in both cases, the total on-chip loss for the PCG is 1.0dB. The

spiral waveguide have a propagation of 6.0 $\frac{dB}{cm}$, the slotted has 14.0 $\frac{dB}{cm}$ and finally a minimum detectable power of 100nW was imposed to our design.

With all these values we obtained a maximum length available to incorporate in our device, which for regular waveguide is 1.10cm and for slotted waveguides is 0.22cm.

We designed and incorporated the spiral photonics wire to the PCG, and this configuration is explained in the Figure 2 - 20

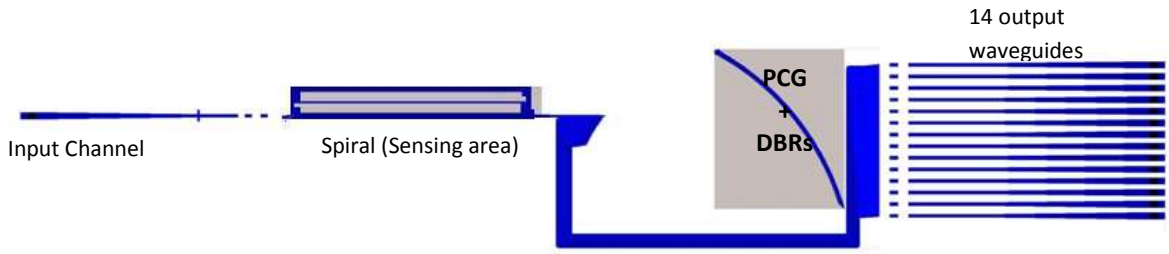

Figure 2 - 20. Scheme of a PCG demultiplexer, with a spiral photonics wire designed as spectrometer-on-a-chip for a Biodiesel blends measurements

With all these parameter founded we uses IPKISS[22] a Python based programming language for generation of GDSII layouts and PICAZZO, a parametric library for photonic components, including waveguides, ring resonators, arrayed waveguide gratings, fiber interfaces, detectors, to create our mask. Our final design contains spectrometers plus and without spiral, spirals as reference and also as sensing tools, and other important devices for our aim. The designed mask is presented in Figure 2 - 21

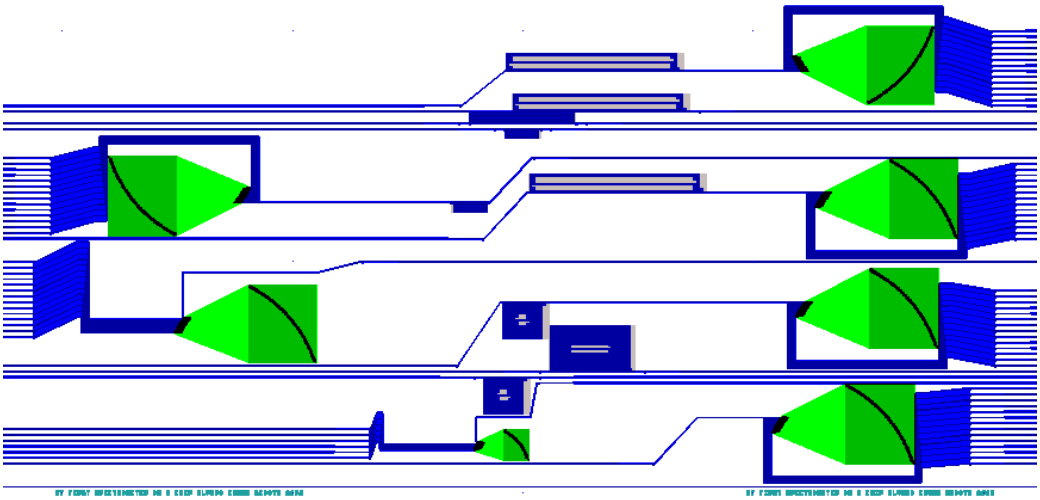

Figure 2 - 21. GDS design used in this work to create the spectrometer able to detect and perform the Biodiesel/Diesel blends absorptions measurement.

As a summary of this chapter, the basic principles behind the SOI arquitectures has been presented, we have described the sources of loss in these devices. Using simulations packages we have found optimum parameters filling the conditions for the task required, and we present the first design realized for a spectrometer-on- a-chip able to perform transmission spectrum measurements for a Biodiesel/Diesel blends.

3. Fabrication.

High-index contrast and highly integrated photonics requires a suitable fabrication technology. The silicon-on-insulator material systems fabricated and discussed in this work is presented in Figure 3 - 1. Consist of a 220nm thick Si waveguide layer on top of 2µm thick buried oxide layer on a Silicon substrate. By etching completely through the silicon waveguide layer, we obtain a very high refractive index contrast leading to a strong confinement.

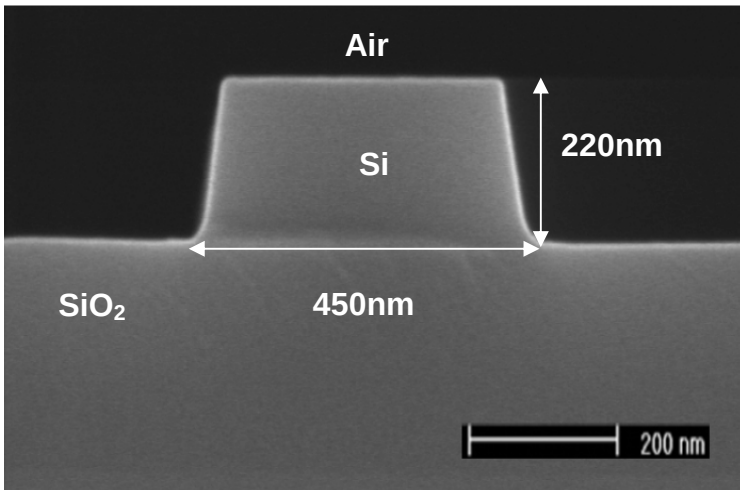

Figure 3 - 1. Electron micrograph cross-section of a photonic wire [19]

In this chapter we describe the fabricated circuit used in this work, also a basic description how the UV photolithography works, the fabrication techniques used for the sensing area implementation, the heaters designed to expand the functionality in our device are explained, and as a final section we compare the GDS designed structure and the fabricated one, including the SU8 opened box.

3.1 Photolithography

Photolithography uses light to transfer a geometric pattern from a photo mask to a light-sensitive chemical photo resist, this is a process used in micro fabrication to selectively remove parts of a thin film or the bulk of a substrate.

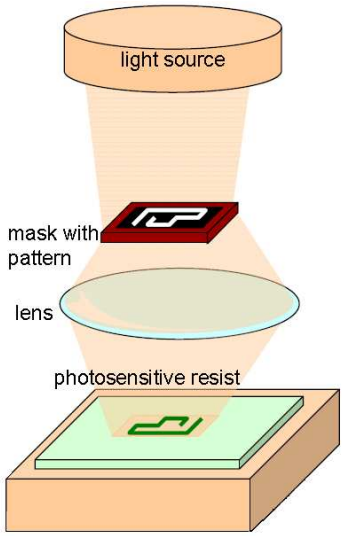

Figure 3 - 2 Schematic draw, showing how to patter a design in a photosensitive resist[23]

The Schematic presented in Figure 3 - 2 shows a photoresist pattern obtained for a mask illuminated by a light source and Figure 3 - 3 depicts the fabrication process overview

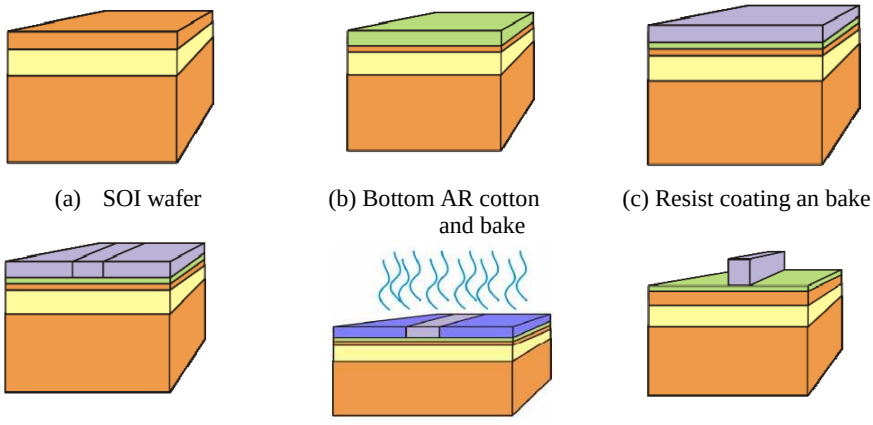

(a) SOI wafer

(b) Bottom AR cotton and bake

(c) Resist coating an bake

(d) Exposure

(e) Post exposure and bake

(f) Development

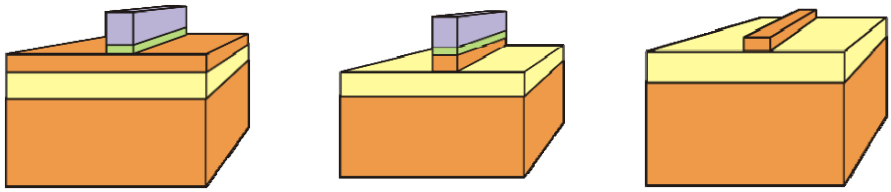

(g) Bottom AR coaching etch (h) Silicon etch (i) Resist and Bottom AR strip

Figure 3 - 3. Lithographic fabrication process flow [19]

The lithographic processes of making a SOI circuit used in this work are described next [19]: We use 200mm wafer scale technology for all of our experiments. The photonic circuits are fabricated on SOI wafers with 2nm of buried oxide and 220nm of top silicon.

- Photoresist application:

  The SOI wafer is first spin coated with bottom antireflective coating (BARC) followed by photoresist. We use chemically amplified photoresist which requires no delay in processing after exposure. Therefore resist process is done on an automated track which is attached to the scanner. After exposure the wafers are baked and developed in the track. The patterned resist is used as an etch mask for silicon etch.

- Exposure and developing:

  For transferring the pattern from reticle/mask to the wafers we use ASML PAS5500/1100 193nm (dry) scanner. The scanner use ArF laser (193) to illuminate the wafer with the reticle image.

- Etching:

  We use ICP-Dry etching to transfer the photoresist pattern into silicon. Lam research Domino is used for dry etching. We use bottom antireflective coating which is insoluble in water and developer solution. Therefore we used HBr/O2 chemistry to etch BARC etch. To etch Silicon we use a combination of HBr/Cl2/CF4/He in three different steps and process condition to achieve profile and dimension control. After etching the wafers the remaining photoresist and BARC is removed by combination of dry and wet etch process

This process is repeated for each designed layer, and complex structures can be obtained.

3.2 Sensing Area implementation

We protected the chip area with SU-8, a photo-definable polymer and rectangular contact windows were opened on top of the sensing area as can be seen in Figure 3 - 4. In addition, a silicone box was also attached to the chip, keeping the fuel inside the open box.

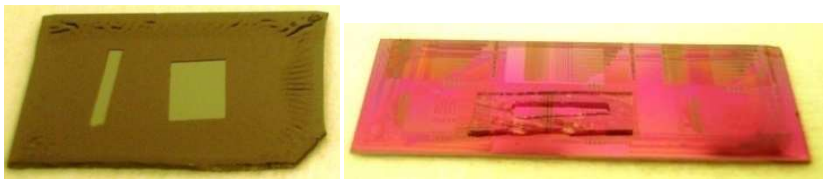

Figure 3 - 4. Photograph of Si plus SU-8 and chip with a Silicone box on top

To be able to perform reproducible measurements, two single mode fibers were aligned and glued on top of the fiber couplers under a 10 degree angle from verticality using an UV-curable glue. This is shown in Figure 3 - 5.

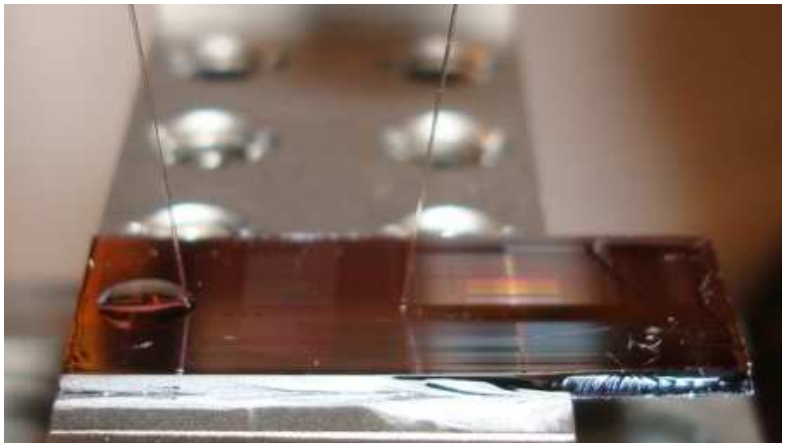

Figure 3 - 5. Picture of the chip and the glued single mode fiber

For the chip characterization we did not glue the exit channel fiber, Instead we use this fiber to measure each of these 14 channels. During the measurements we cleaned the chip by first removing the exit optical fiber and then using acetone and Isopropanol to clean the surface that was exposed with the fuel.

3.3 Heater on SOI-waveguide circuit

Silicon waveguide circuits are very sensitive to temperature; therefore by rising the temperature of the SOI circuit the refractive index of the material change and as a result the output focused wavelength form the grating will be also changed.

This can be done by growing a thin layer of BCB on top of the SOI chip, and adding two metal contacts joined by a metal path. This path is transporting a given current between the contacts and will heating the BCB layer, thus the SOI will be also heated leading to a refractive index change.

We designed a mask for the heater and are presented below in Figure 3 - 6.

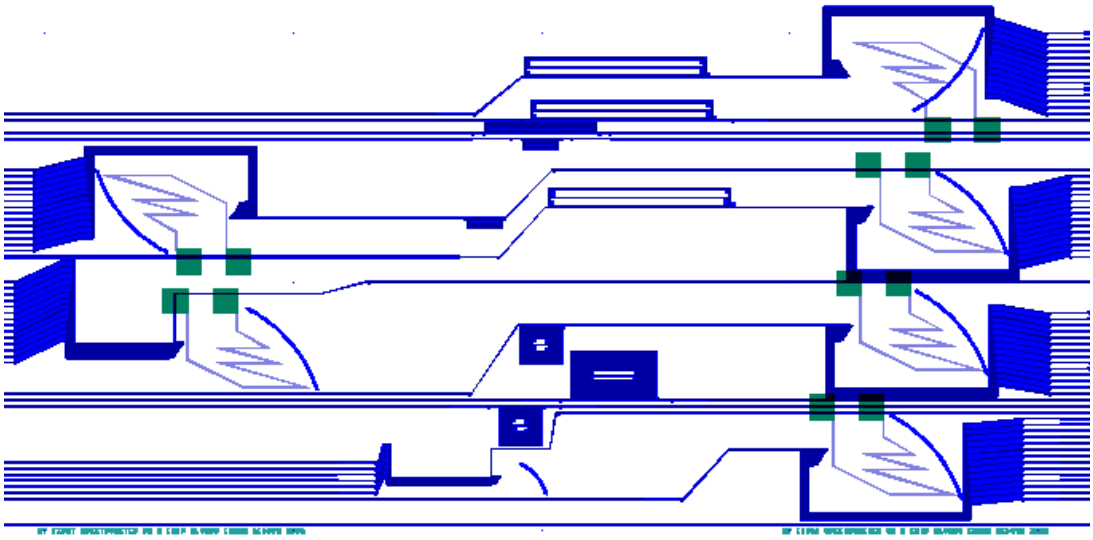

Figure 3 - 6. GDS schematic for the heater designed for this work (heaters in dark green)

Although this heaters mask was fabricated we did not used it, because the design was developed for the positive layout and the fabricated was a negative layout. Therefore we needed to incorporate another fabrication step in the process.

3.4 Fabricated circuit.

The SOI waveguide circuits were defined with 193nm deep-UV lithography and transferred into the silicon using ICP-RIE etching. For the definition of the grating demultiplexer, the photonic wire and slotted waveguides, we etched completely through the 220 nm thick Si

layer. A more shallow etch (70 nm) was used for the definition of the 2 μm wide entrance and exit waveguides of the PCG[7]. In the shallow etch step we also defined grating fiber couplers which allow for easy characterization[14]. The fiber couplers are one dimensional grating which allow to couple nearly vertical incident light from a standard single mode fiber into the nanophotonic SOI waveguides.

The fabricated DBRs have four periods of 682.2 nm in total, a trench width of 145 nm and an unetched part of 542.2nm. Figure 3 - 7 is a top view photograph of a part of the grating and Figure 3 - 8 is a SEM picture of one DBR facet.

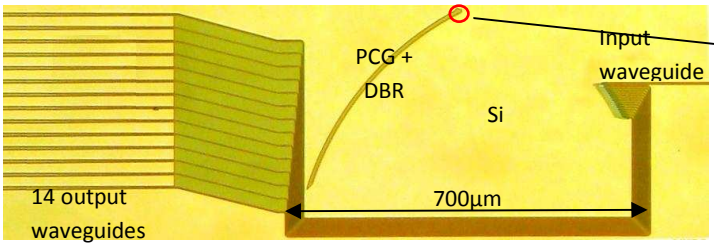

Figure 3 - 7. Microscopic photograph of the fabricated SOI - PCG with 14 channels and DBR

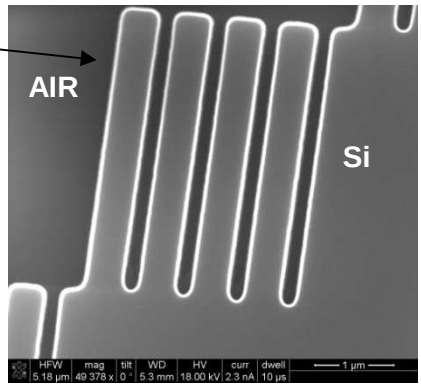

Figure 3 - 8. SEM Top view of DBR-type grating facets, with a width of 145 nm. The unetched part is 542.2nm wide

The PCG demultiplexer has one input waveguide and 14 output waveguides. The size of the diffraction grating, consisting of 91 facets totally, is about 440μm.

Finally Figure 3 - 9 compare the designed SOI chip containing all our structures and the fabricated. The fabricated differs from the designed one by a mirrored effect and we have called the GDS layout, positive and the fabricated layout, negative.

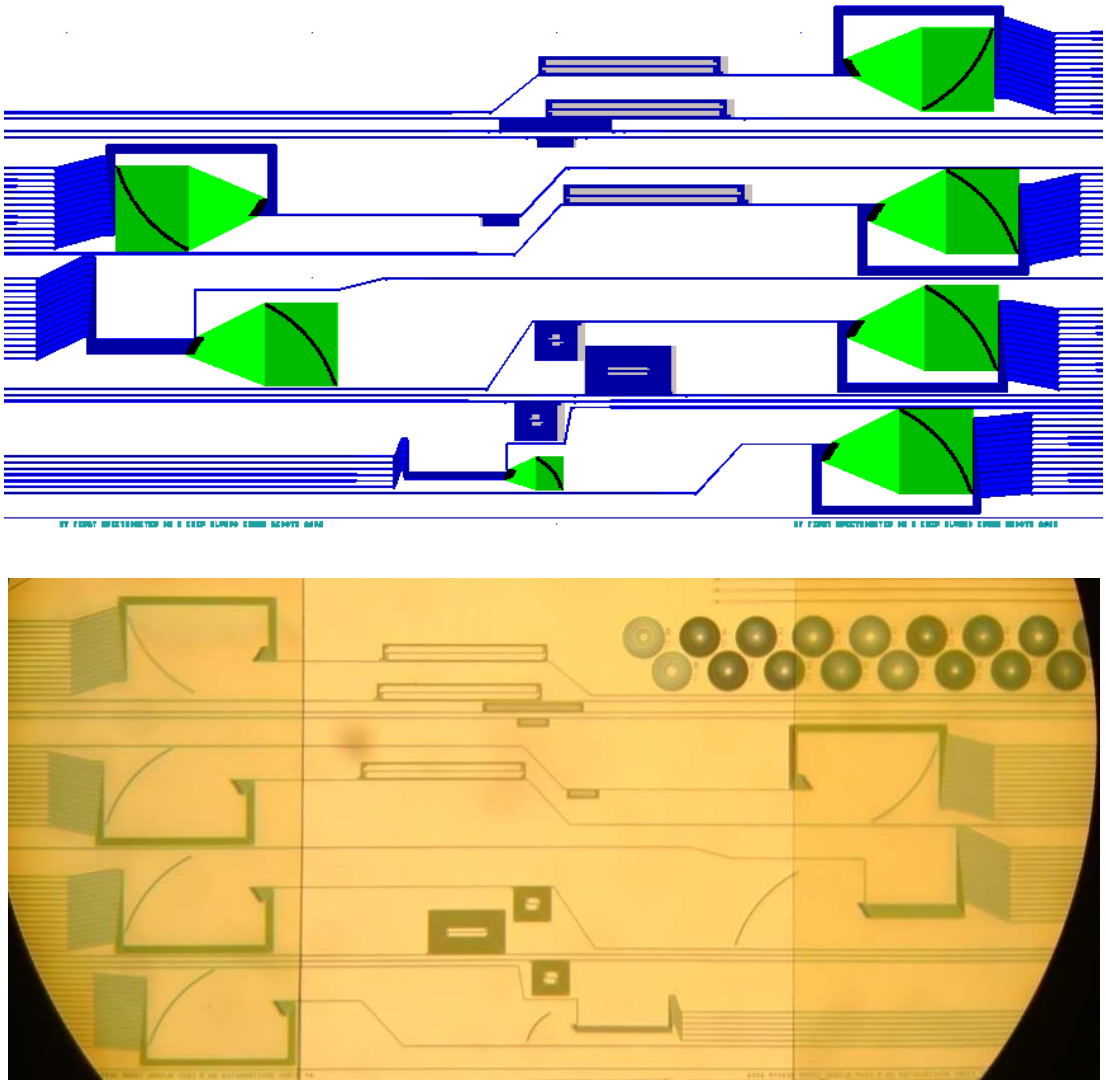

Figure 3 - 9. Comparison between GDS design (Positive) and fabricated SOI chip with a SU8 box on top (Negative).

Using photolithographic technique it is possible to fabricate a High-index contrast and highly integrated photonics. We have fabricated a Silicon-on-insulator structure designed to fill the requirements for a Biodiesel sensor application.

We create a sensing area to be in contact with the fuel and to feel the absorption processes. We integrate successfully a SU8 box able to keep the fuel inside on our sensing area and isolating the chip for a possible fuel spreading.

4. Measurements & Results.

The experimental setup used to characterize the sensor structure and to take all the measurement is presented in Figure 4 - 1. In this setup, two single mode fibers are aligned on top of fiber couplers under a 10 degree angle from verticality. These fiber couplers allow to couple light from the fiber into the chip and vice versa [(14)].

For the first characterization experiments, we measured the transmission spectra on existing chips with an Optical Spectrum Analyzer (OSA) with resolution setting of 0.1nm. We used as a light source a Superluminescence Broadband Light Emitting Diode (SLED) with a center wavelength at 1550nm, and for the spectrometer-on-a-chip that we designed we used a SLED centered on 1650nm, which corresponds to the Biodiesel/Diesel blends absorption.

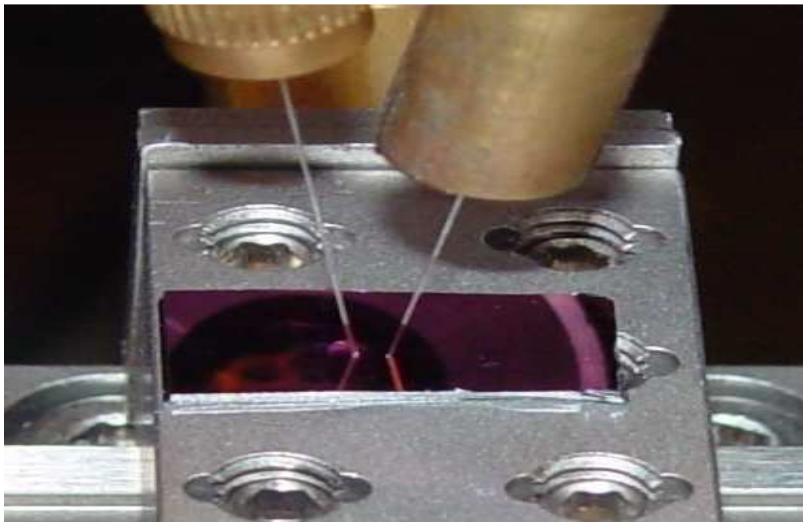

Figure 4 - 1. Picture of the chip and the single mode fibers aligned in the chip

In this chapter, we will discuss the measurements we performed. These measurements include the characterization of the individual components such as the spiral waveguides and the PCG demultiplexer, and the fuel absorption measurements using these spirals in combination with both the OSA and the 14 channel spectrometer-on-a-chip.

4.1 Spiral waveguide characterization using a 1550nm SLED

As a first approximation to our sensing structure we used a set of existing spirals photonics wires optimized for 1550nm. We measured the propagation losses and the interactions between the fuel blends and photonics wires with a SLED centered on the same wavelength.

4.1.1 Spiral waveguide characterization

We measured the transmission spectrum of a set of four different spirals with lengths from 6.394mm up to 41.394mm. These transmission spectrums are presented in Figure 4 - 2, and the linear behavior observed in Figure 4 - 3 was obtained by taking the maximum power transmitted for each spiral. With the linear regression we compare the losses and we calculated a propagation loss of 3.03 ± 0.03 $\frac{dB}{cm}$ for the wires.

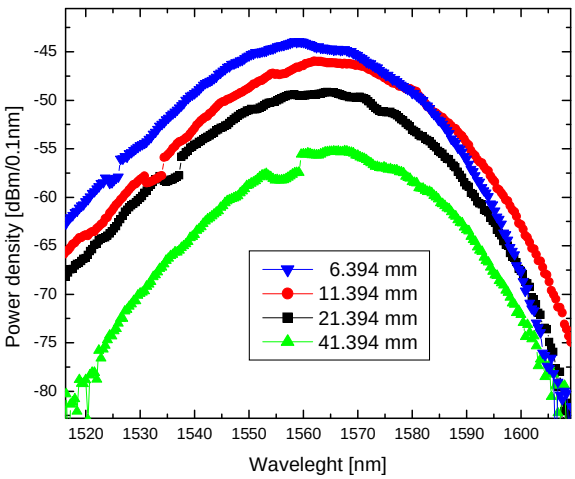

Figure 4 - 2. Transmission spectra for spiral shaped photonic wire waveguides with different lengths ranging from 7mm to 41 mm.

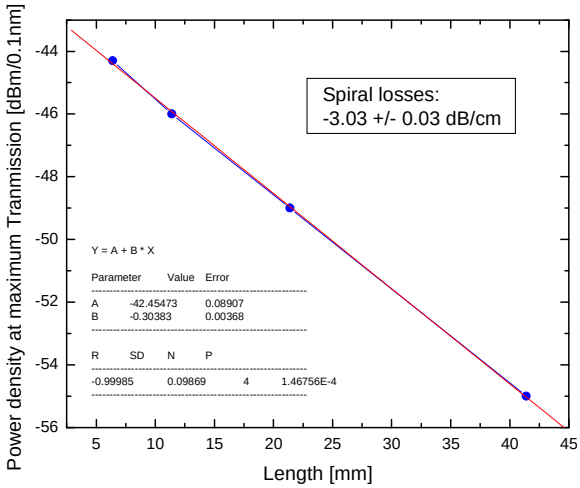

Figure 4 - 3. Propagation losses for a set of five different spirals.

We also measured the transmission spectrum after the incorporation of the sensing area. Here the effect of the SU8 on top of the grating couplers and photonics wire structures

produces a shift to all the transmission spectrum of 5nm towards longer wavelengths. We added manually the fuel by adding a drop on top of the chip and we found that the transmission spectrum shift again nearly to its original position (Figure 4 - 4.)

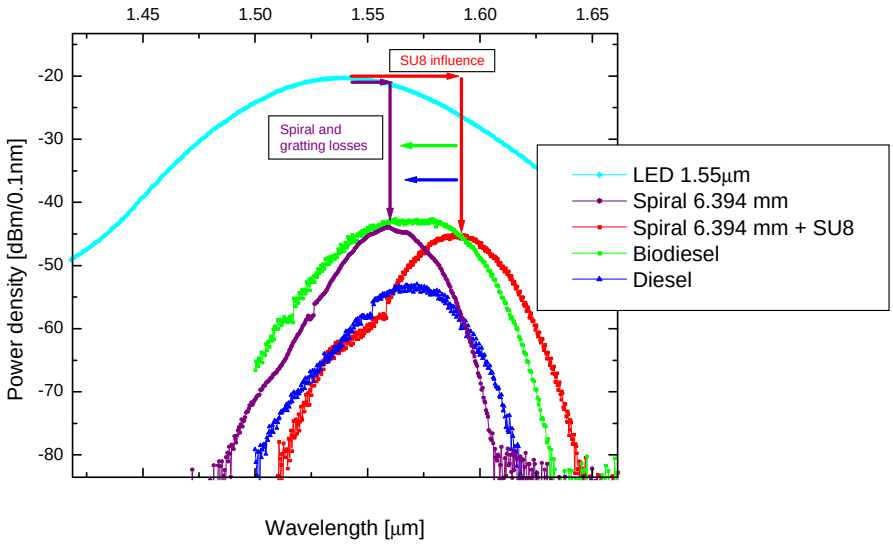

Figure 4 - 4. Transmission spectra for a 1550nm SLED (Clear Blue), 6.394 mm spiral shaped photonic wire waveguides (Purple), plus the SU8- sensing area design (Red), and the fuel additions (Green and Blue)

When we added the fuel on top of the chip we observe a small leak from our sensing area and therefore the fuel get in contact with the grating couplers, for that reason we attribute the shift in the transmission spectrum to this change in the coupling efficiency and refractive index contrast between these materials, as a solution to this leak we decide to glue the optical fibers using a photo curable UV Glue. The glue protects and covers both the grating coupler and the optical fiber

4.2 Sensing Biodiesel using spiral shaped waveguides

As mentioned earlier, the goal of these measurements is to investigate the possibility to determine Biodiesel blend levels by measuring the transmission through different waveguide configurations. For these experiments, we fabricated spiral shaped 500nm wide photonic wire waveguides with different lengths. The fuel was added manually on top of the sensing box, as is shown in Figure 4 - 5.

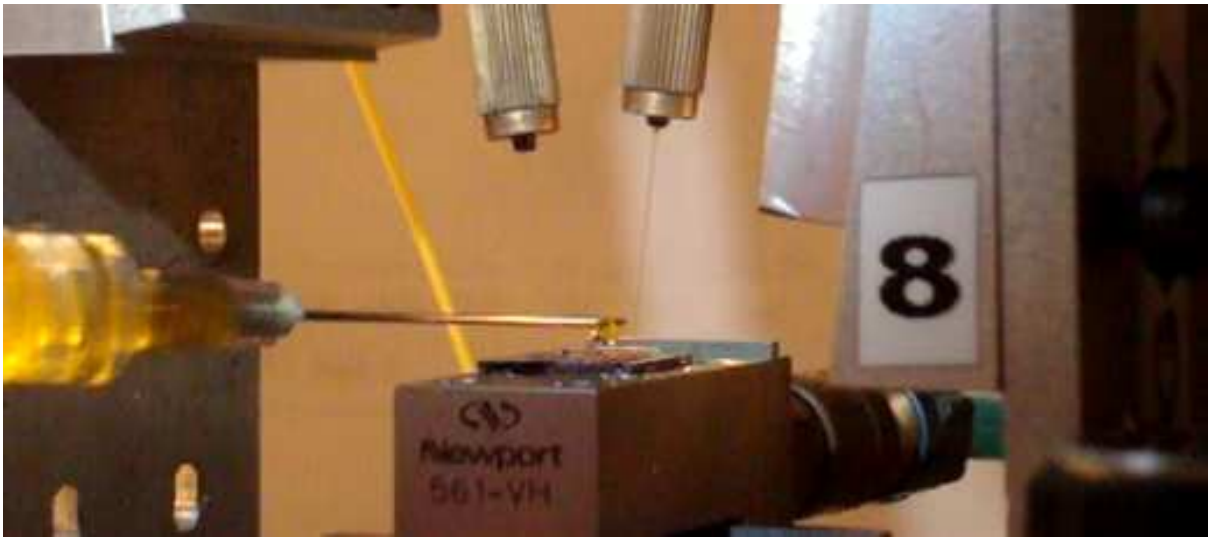

Figure 4 - 5. Set up Photograph and fuel addition using a syringe.

The transmission spectrums from the chip were measured with an Optical Spectrum Analyzer (OSA) with resolution setting of 0.1nm. And we used the SLED centered at 1650nm as the light source.

4.2.1 Spiral waveguide characterization

We measured the transmission spectrum of a set of four spirals with different lengths. (Figure 4 - 6). The small oscillations are due to Fabry-Pérot effects caused by reflections at the fiber couplers [14] The linear behavior observed in Figure 4 - 7 was obtained by taking the maximum power transmitted for each spiral. With the linear regression we compare the losses and we calculated a propagation loss of 5.80 ± 0.27 $\frac{dB}{cm}$ for the wires without Biodiesel on top.

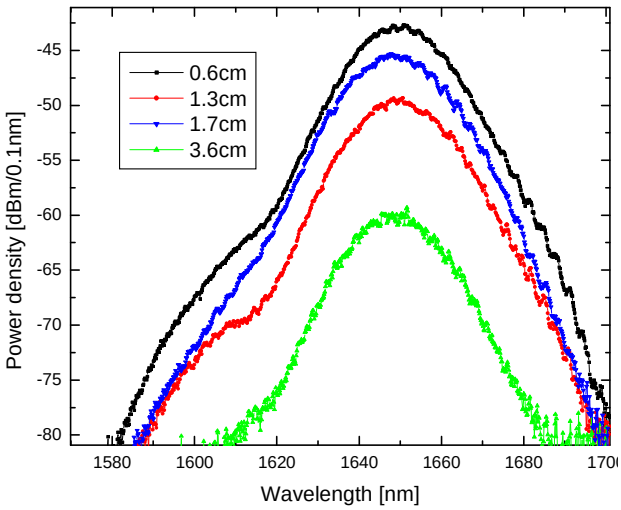

Figure 4 - 6. Transmission spectra for spiral shaped photonic wire waveguides with different lengths ranging from 7mm to 36 mm.

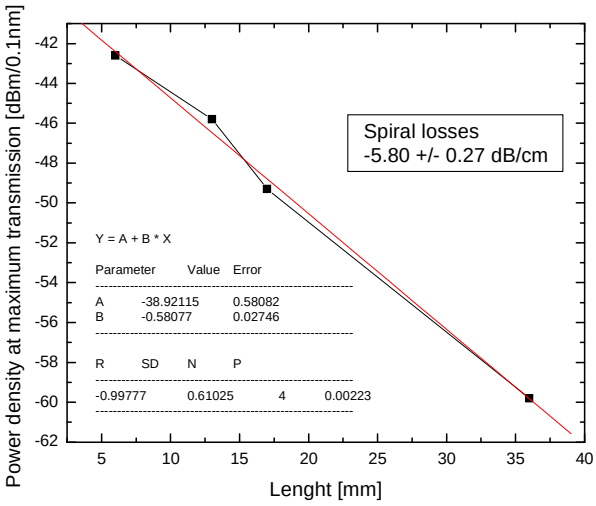

Figure 4 - 7. Propagation losses for a set of four different spirals.

We found that these losses are higher than the previous ones for the spirals optimized at 1550nm. This is explained due to the SiO_2 infrared absorption. The oxide layer for wavelength longer than 1600nm becomes highly absorbing and thus, more light from the Si core is extracted.

4.2.2 Sensing the Biodiesel blends.

Each photonic wire waveguide was tested with different kinds of Biodiesel/Diesel blends. As mention previously the different fuels were added manually on top of the sensing box. Here using equation 2-2, we predicted the behavior of the spiral with the fuel on top; this model uses the measured transmission for pure Biodiesel and pure Diesel shown in Figure 1 - 1 and the confinement factor of each structure (20% for regular waveguides).

As a comparison we present in Figure 4 - 8 (a) the fuel absorbance for pure Diesel and pure Biodiesel and in Figure 4 - 8 (b), the predicted transmission obtained, using this absorbance and the model described in chapter II.

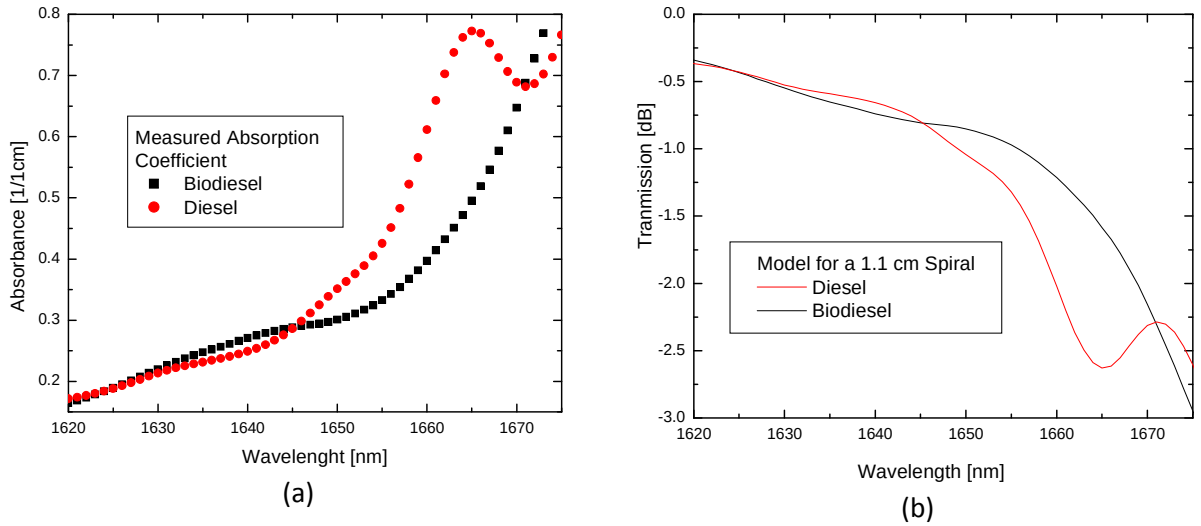

Figure 4 - 8. (a). Biodiesel and Diesel absorbance, (b) Predicted transmission spectrum for a 1.1cm spiral photonics wire.

We found agreement with the higher wavelengths absorption i.e. less transmission. Moreover the crossing of both lines for 1630, 1645 and 1670nm are related with the absorption properties for both fuels. We found that for these points the absorption coefficient has the same value.

Each measurement sequence consists of two parts. First, we measure the transmission spectrum of the spiral waveguide without fuel on top of the sensing area. Secondly, we measure the transmission after we added a fuel mixture on top of the sensing area. Finally, the transmission is normalized by subtracting both measurements. This way, the normalized spectrum already takes into account the waveguide propagation loss.

The experimental measurements are shown in Figure 4 - 9, together with the simulated transmission. As can be seen, the measured transmission is about 2dB higher than the modeled transmission. This is due to influence of the presence of the fuel on the waveguide scattering losses [24].

The lower index contrast obtained from (Biodiesel–SOI) in comparison with, (Air–SOI), reduces the propagation losses. The Fuel has higher index than air, thus less waveguide confinement and smaller light intensity at the edges is achieved, therefore the light feels less the presence of roughness along the edge of the waveguide and travel trough the Si core in an efficient way.

To solve this fact and to obtain a better visualization in our results, we have subtracted to the measured spectrum, the difference between the model and the experimental result, and we

took the 1670nm point as a reference, because the transmission spectrum for both fuels has the same value in this point. We found a reduction due to scattering losses of 2.1dB.

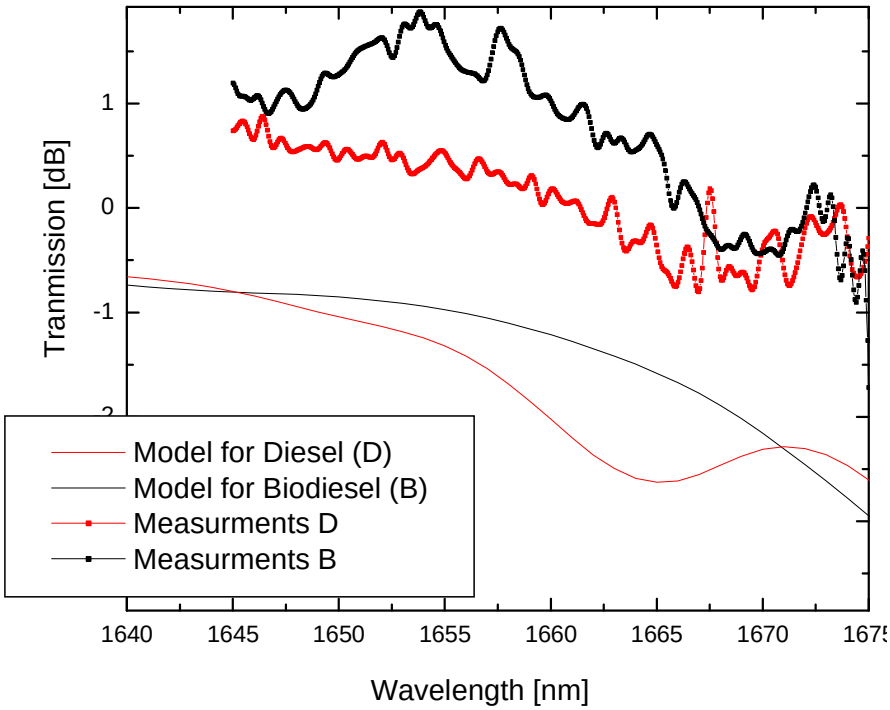

Figure 4 - 9. Measurement and model comparison for the Biodiesel Diesel transmission spectrum for a 1.1 cm long spiral

After the scattering losses subtraction, Figure 4 - 10 plots the theoretical and the measured transmission of a 1.1 cm spiral. Here we found good agreement between model and measurements, and the differences in transmission between wires with standard Diesel and with Biodiesel are in the order of 2 dB for the 1665nm region. The oscillating behavior is attributed to the Fabry-Pérot behavior found also in the spiral characterization

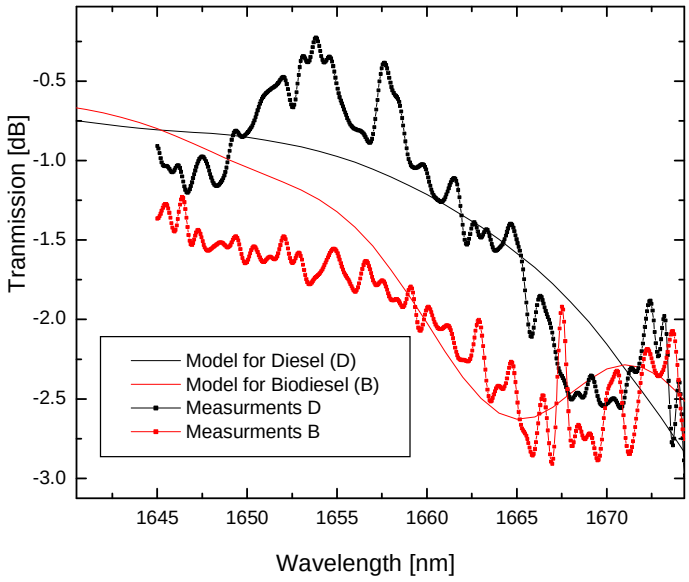

Figure 4 - 10. Measurement and model comparison for the Biodiesel Diesel transmission spectrum for a 1.1 cm long spiral after scattering losses subtraction

We carried out a second experiment with the 1.1cm long spiral, to confirm our results (Figure 4 - 11), but in this case we create an unknown Diesel/Biodiesel blend by adding a drop of pure Biodiesel on top of an existing Diesel in the sensing box. As expected, the difference between pure Diesel and the blend decreases but is still clearly visible.

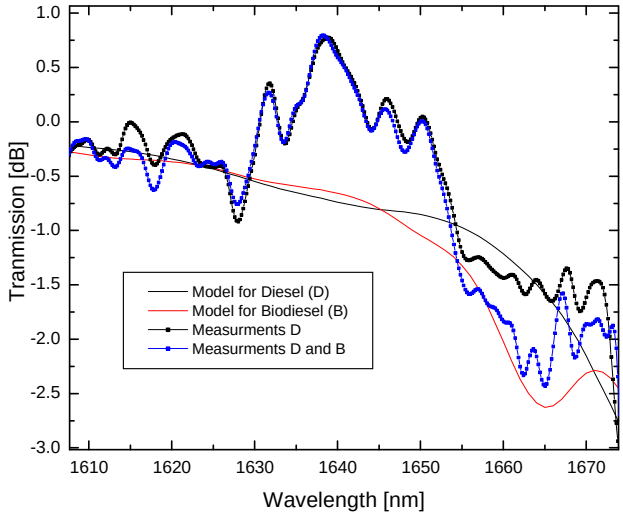

Figure 4 - 11. Measurement and model comparison for the Diesel – Blended Diesel transmission spectrum for a 1.1 cm long spiral.

Finally a 3.6cm spiral was analyzed and is presented in Figure 4 - 12. Again, the measurements agree with our expectations and the differences in absorption are around 4dB (at 1665nm), making possible the identification of the fuel composition.

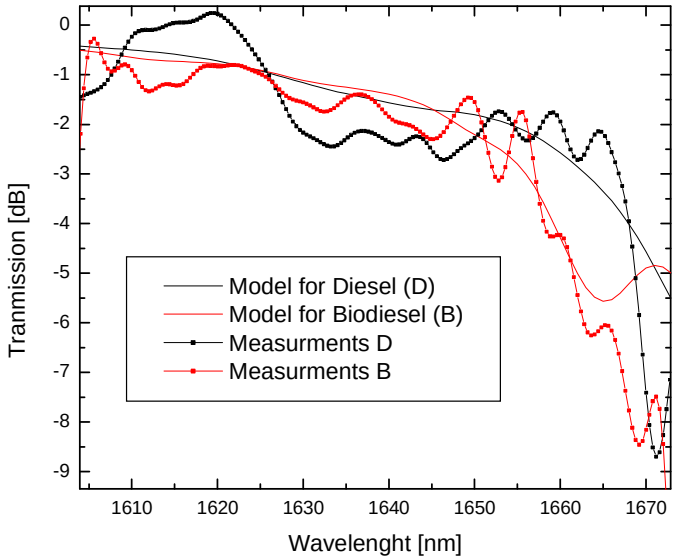

Figure 4 - 12. Transmission spectrum measurement, and model comparison for a 3.6cm spiral plus Biodiesel and Diesel

4.3 Sensing Biodiesel using a 14 channel planar concave grating demultiplexer.

The integration of SOI structures and a PCG as a fuel sensing arquitectures are the aim of this work. Here we get closer to the goal of this project, which consists in the use of a miniaturized spectrometer able to perform Biodiesel/Diesel blends measurements and bring to the market a cheap, small and reproducible easy handling device.

4.3.1 Planar Concave Grating demultiplexer characterization.

For the characterization of the chip we also used the set up mention previously, and the drop of the fuel was also added manually in to the chip. For this characterization, we measure the transmission spectrum of a straight waveguide, and secondly we measure the transmission of each channel. The transmission measurements were normalized by subtracting both measurements, in this way the normalized spectrum already takes into account the waveguide propagation and the grating couplers losses, and give us the diffraction and the reflection losses which are known as the total on-chip losses.

We characterize the 14 Channel PCG; and the normalization was done for each of the 14 channels, thus, we obtain the 14 channel PCG characteristic spectrum which shows us the

total on-chip losses. The simulation performed and presented in Figure 2 - 13, is then compared with the measured values, and are presented in Figure 4 - 13.

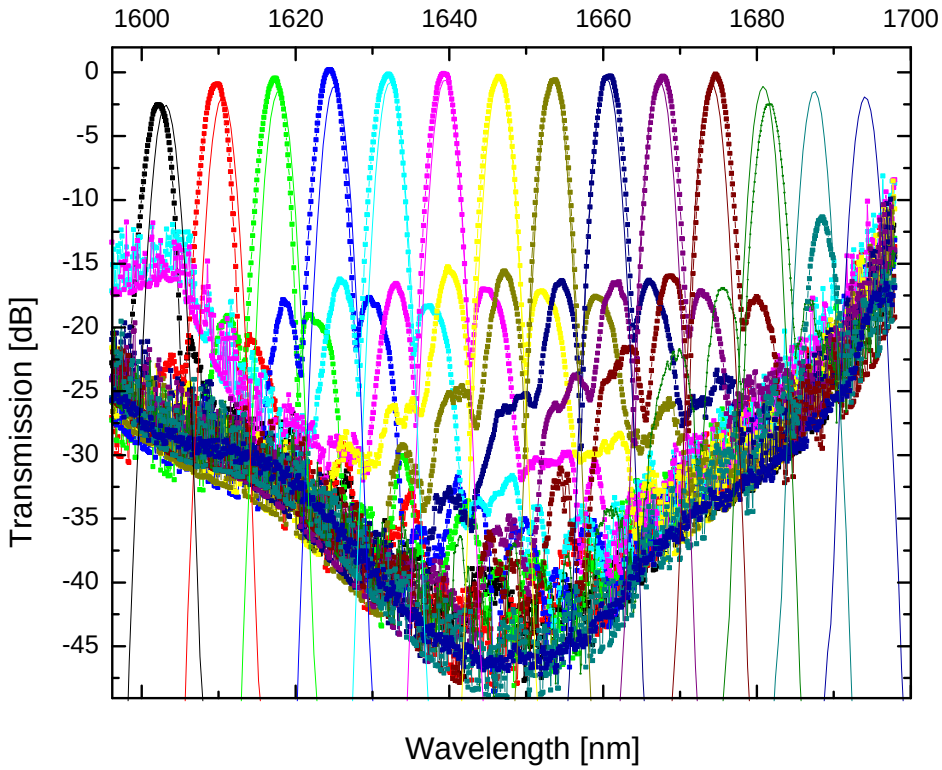

Figure 4 - 13. Transmission spectrum measured for a 14 channel demultiplexer and simulation comparison

In concordance with our simulation we found 7 nm of channel spacing and a good response for almost all the channels, however the last two channels at the right of the characteristic PCG transmission spectrum were difficult to measure due to the noise floor and the propagation losses incorporated by the 1.1cm spiral, but they are out of our interest because the blends obtained using only the spiral shows us that the big differences are centered around 1610 and 1670nm.

The simulation discussed in the previous chapter shows diffraction losses of about 0.5 dB for the central channel (1650nm), also 30dB crosstalk, and 0.5dB due to the DBRs. The measurements obtained show an improvement in the total on chip losses, and we obtain 0.46dB more than the simulated for the central channel. The crosstalk is better than 15dB as is presented in Figure 4 - 14.

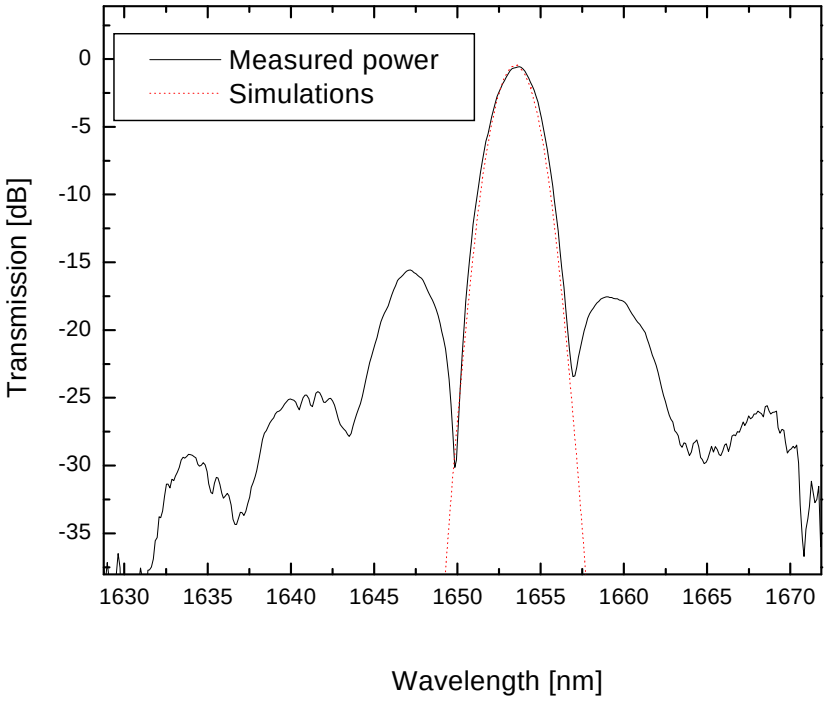

Figure 4 - 14. Transmission spectrum comparison between an ideal channel response and the measured one.

We obtain higher values for the transmission spectrum, than the simulated ones, which only take in account the diffraction losses, most probably because we have a very long photonic wire, whereas the input of the PCG is maybe a very short wire. Therefore the straight waveguide which works as normalizing tool incorporating losses can also show an apparently improvement in the efficiency for our device.

On the other hand the lithographic exposure doses will results in a different width of the deeply etched trenches. This has a major influence of the transmission spectrum of the DBR grating facets as is was explained in section 2.2.3. In our case the simulation showed for the central channel, diffraction and reflection losses of 1dB, values which were obtained in our measurements for 24 $\frac{mJ}{cm^2}$ dose. The transmission spectrums for the PCG central channel were taken for different doses and are plotted in Figure 4 - 15. This characterization showed us that for a 26 $\frac{mJ}{cm^2}$ dose the diffraction and reflection losses are both improved by 0.4dB in comparison with our design which uses 24 $\frac{mJ}{cm^2}$ dose.

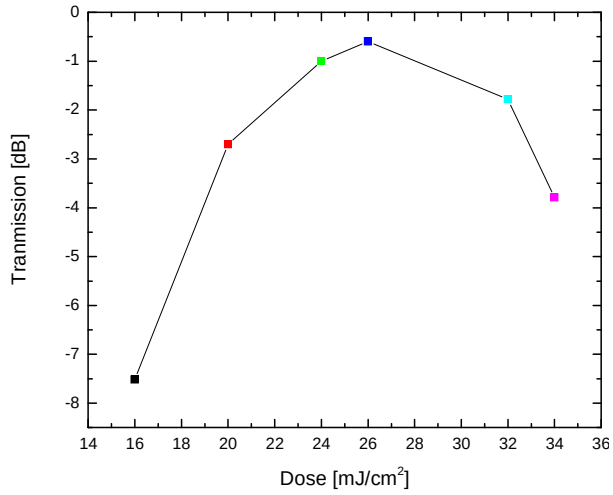

Figure 4 - 15. Maximum transmission spectrum for the PCG central channel versus exposure doses

Using this reasoning and the value obtained from the measurement, the consequent experiments were realized using the chip which was exposed to 26 $\frac{mJ}{cm^2}$

As a reference in our design we incorporate a PCG with a flat reflecting facets, this was also done to avoid any possible mistake in the parameters imposed to the DBR widths. The improvement achieved by adding the DBR was around 5dB for each channel, the measured values are compared in the Figure 4 - 16 .

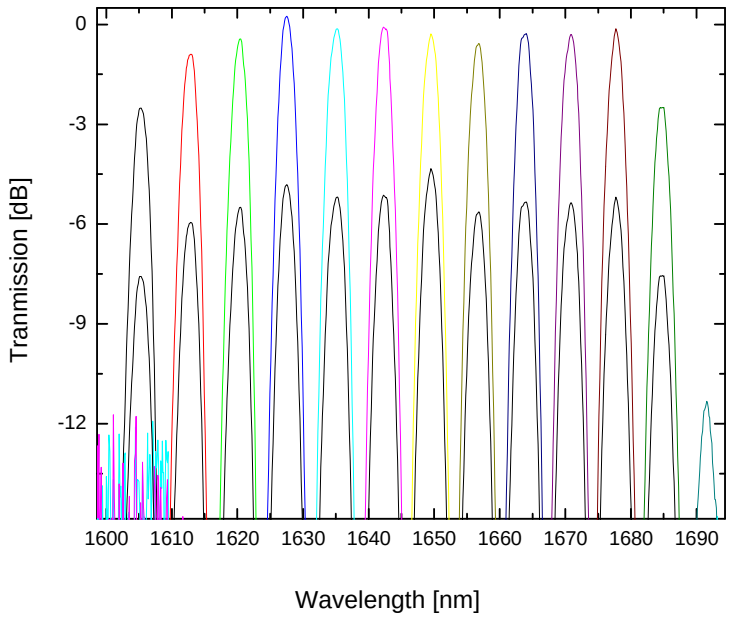

Figure 4 - 16. Transmission spectrum of a 14 demultiplexer, Demultiplexer with flat (black line) and DBR-type facets are compared.

4.3.2 Sensing the Biodiesel blends.

As a final part of this work we measured the Fuel blends using the PCG plus the 1.1 cm spiral designed for that propose. In these measurements we manually added a fuel drop in the sensing box and the procedure to obtain the spectrum was similar as the used to characterize the spectrometer, with the differences, that here we use the 1.1 cm spiral reference as a normalizing tool, the spectrum was taken using the OSA with resolution settled at 0.5nm and we glued the optical fiber into the input channel after the spiral characterization.

Figure 4 - 17(a) plots the fiber-to-fiber power density transmission spectrum for a 1.1 cm spiral photonic wire and the 14 Channels PCG plus this spiral without gluing the optical fiber.

Figure 4 - 17(b) presents the fiber-to-fiber power density transmission spectrum only for 3 channels from the 14 channels PCG plus a 1.1 cm spiral. Here the PCG was implemented as a spectrometer-on-a-chip for a Biodiesel sensing application by adding the sensing area that we design and by gluing the input optical fiber.

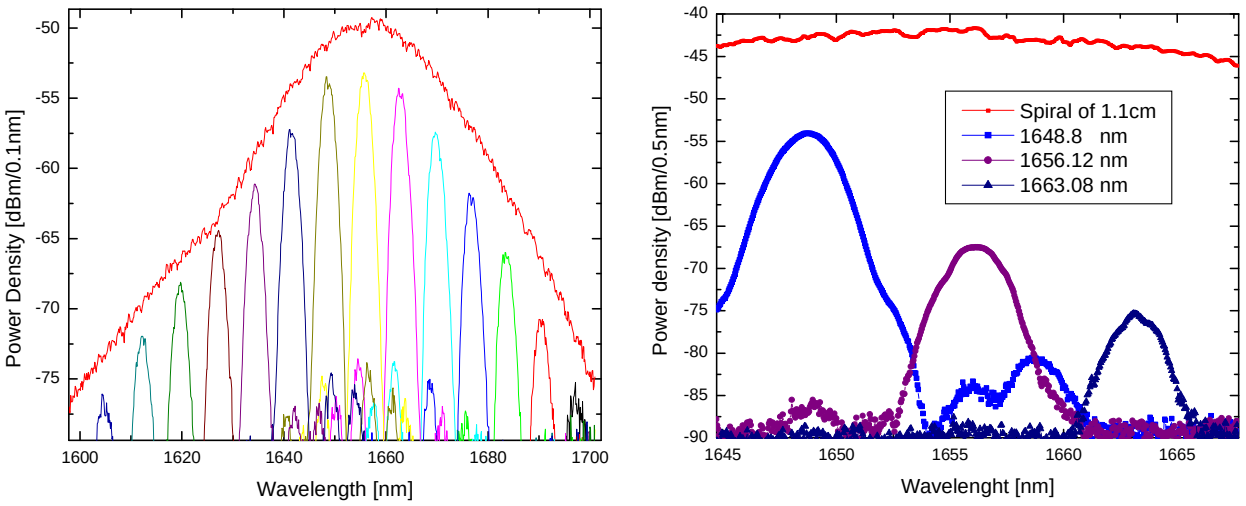

(a) (b)

Figure 4 - 17. (a) Power density transmission spectrum for a 14 Channels PCG plus a 1.1 cm spiral. (b) 3 channels Power density transmission spectrum from a 14 Channels PCG with a 1.1 cm spiral implemented as a spectrometer-on-a-chip for a Biodiesel sensing application.

We believe that here the decrease in the power density for longer wavelength is due to the SU8 box added to the chip and we also observe that the grating coupling efficiency decrease after we glued the optical fiber into the input channel.

Figure 4 - 18 compares the transmission spectrum for pure Diesel and pure Biodiesel for the three channels presented previously. These three channels correspond to the higher fuel absorption region, the differences obtained for the Diesel and the Biodiesel has for all of the points correspondence with the differences observed in the Biodiesel/Diesel blends transmission spectrum (Figure 1 - 1) and in with the model which predicts the absorption behavior (Figure 2 - 19)

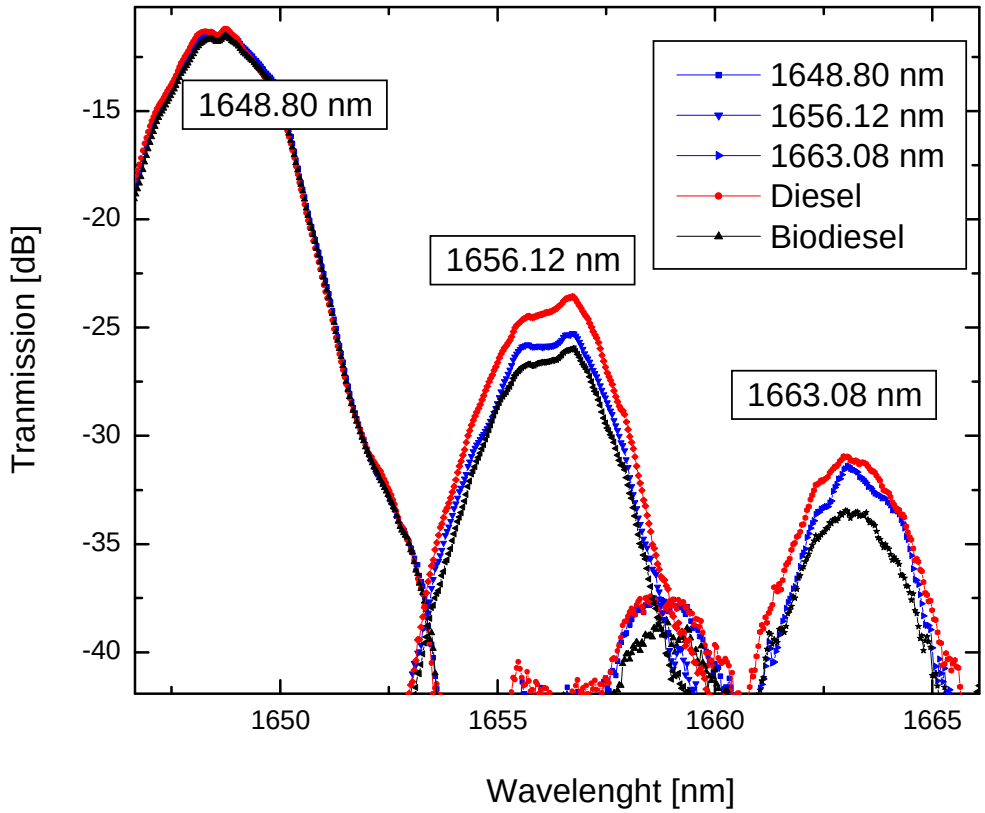

Figure 4 - 18. Three channels Blends measurements using a 14 Chanel PCG.

But, for a better observation from this last results and as a final goal of this project we did not use the OSA, instead we used a power meter with resolution of ±2 nW for high power channels and ±5 nW for low power channels.

We measured the power at the 8 central channels from our spectrometer-on-a-chip, thus we achieve the maximum absorption from the blends. In this experiment we add pure Diesel, pure Biodiesel and a 50/50 blend solution in to our sensing area. These measurements are presented in the Figure 4 - 19

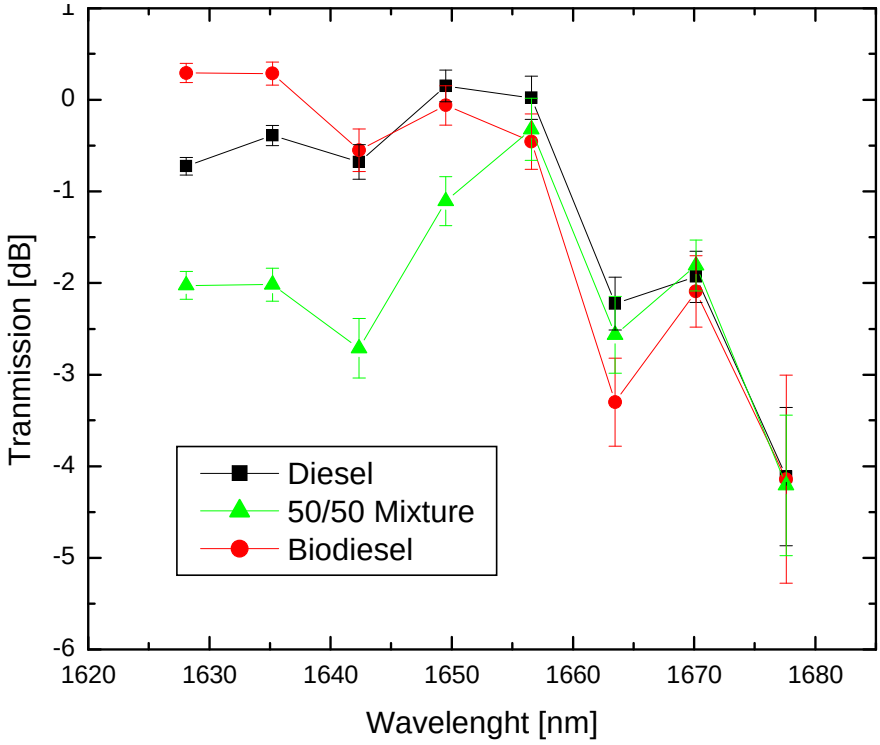

Figure 4 - 19. Biodiesel/Diesel Blends measured with a power meter using a 14 Channel PCG plus 1.1cm Spiral as a sensing tool.

Again the Scattering losses are important in these measurements. We consider the values above 0dB and we define a reference point. We took again the 1670nm shared point for both measurements and the scattering losses were considered around 2dB as in previous results. On the other hand the 50/50 mixture (green line), is beyond the limits before 1650nm, definitely for the values minor to 1650nm, something went wrong, we have attributed this behavior probably due to a low coupling efficiency caused by a shift in the input fiber during cleaning process.

To understand the last graph, we compare the differences in transmission between pure Diesel and pure Biodiesel by means of absolute difference, for the predicted and measured values and we call these differences ΔFuel. (Figure 4 - 20)

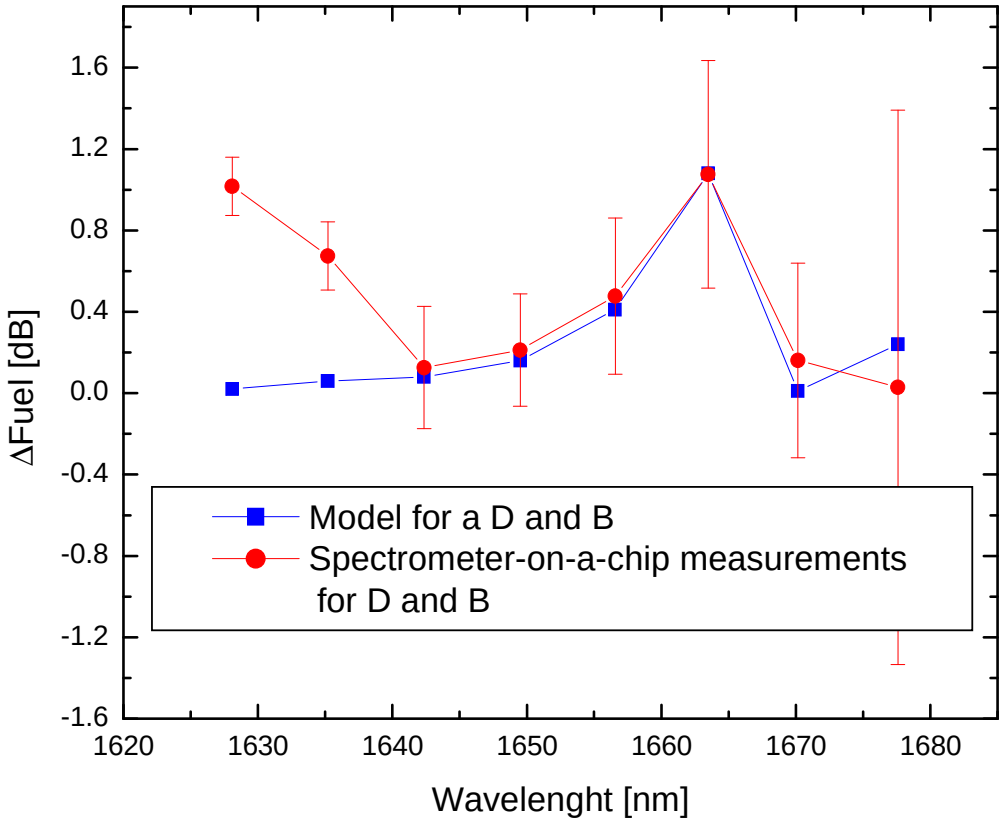

Figure 4 - 20. Model and measured transmission spectrum differences between pure Diesel and pure Biodiesel for 8 different channels in our spectrometer-on-a-chip.

The previous graph shows how the differences between pure Diesel and pure Biodiesel can be used as reference for blends identifications, moreover the agreement founded shows the how our model is working in concordance with our expectations.

The long error bars in our measurements are caused due to the low power coming out form the corresponding channels. Again due to cleaning process we observe that for the first two channels the measurements are not accurate.

Finally we also compare the difference in transmission between Pure Biodiesel and the 50/50 Blend. Figure 4 - 21 excludes the first four channels because we already saw that something went wrong during the measurements, but the important fact here is that we prove that we are able to sense the Biodiesel/Diesel blends using SOI structures.

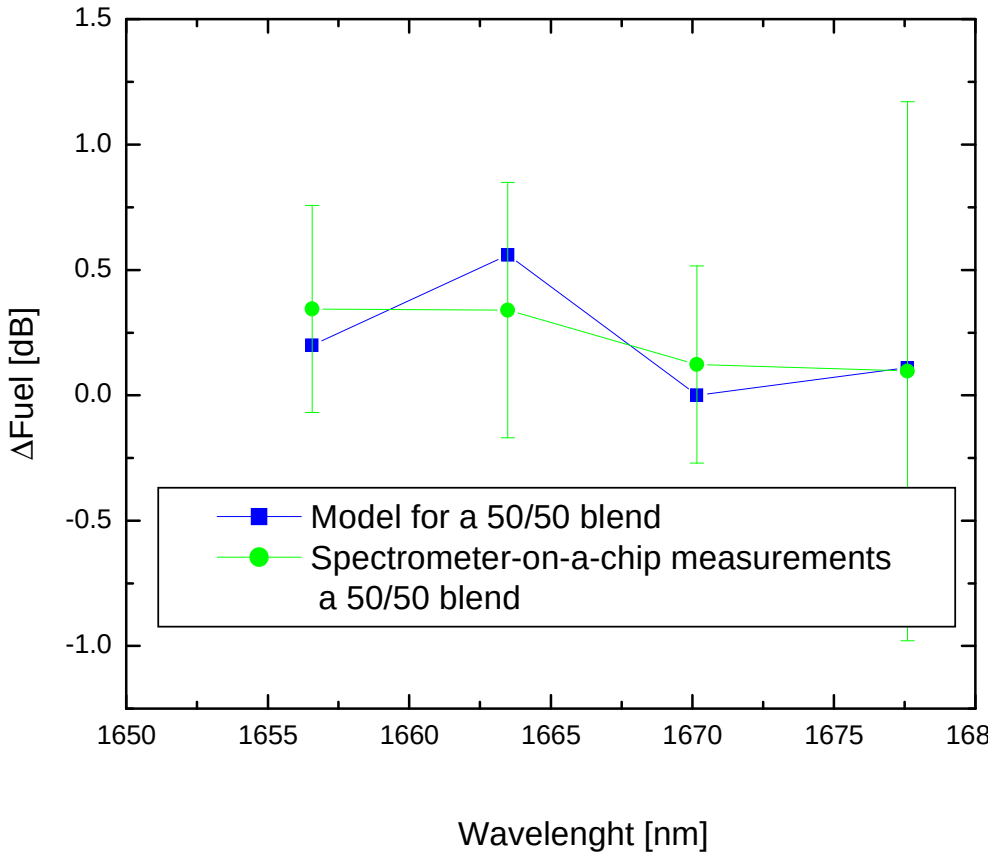

Figure 4 - 21. Model and measured transmission spectrum differences between pure Biodiesel and a 50/50 blend for 4 different channels in our spectrometer-on-a-chip.

Now by considering all the 14 channels and using a multivariate analysis[3], the spectrum or the values measured in the previous graphs can be related to the change in blends concentration, and in addition this technique also involves more than one wavelength, exactly as in our case for all the 14 exit channels from our spectrometer-on-a-chip.

As a conclusion in this chapter we integrate all the study developed in order to sense the Biodiesel blends and we prove that using SOI arquitectures this analysis can be reliable, moreover important facts as the scattering losses, Fabry-Pérot reflections in the grating couplers, the fuel interaction with the material and the accuracy in the measurements will determine the final spectrum and the fuel absorption characteristics.

.

5. Conclusion.

The basic principles behind NIR absorption spectroscopy including a SOI structures are presented in this study. We describe the sources of loss in the SOI devices used. Using simulations packages, we were able to determine the optimal parameters allowed for the effective measurement of the fuel blends.

With deep UV photolithographic techniques, it is possible to fabricate a High-index contrast and highly integrated photonics. We have shown Silicon-on-insulator spiral shape waveguides are able to sense the absorption of Biodiesel/Diesel blends and can incorporate these spirals successfully with the planar concave demultiplexer. Thus, the PCG and the spirals fabricated act as spectrometer-on-a-chips, sensing the blends at different wavelengths.

Using the fabricated spectrometer-on-a-chip with the 1.1cm spiral, we measured the transmission spectrum for pure Diesel, pure Biodiesel and a 50/50 blend. For a particular point in the high absorbing region, (1663.48nm), we predicted 1.08 dB and we measured 1.075 ± 0.559dB for the difference between Biodiesel and Diesel, and for the 50/50 blend, we predicted 0.56dB and we measured 0.339 ± 0.509dB for the difference between pure Biodiesel and the 50/50 blend.

With the fabricated device we show and demonstrated important factors influencing this absorption and sensing process, including; the scattering losses, Fabry-Pérot reflections in the grating couplers, the fuel interaction with the material, the accuracy of measurements in determining the final spectrum, and the fuel absorption characteristics.

Perspectives

- The addition of a flow cell or a tube transporting the fuel into the sensing area should be implemented.
- The scattering losses should be studied in detail to achieve better accuracy in the measurements.
- The use of more than one spectrometer is recommended to sense the blends in the final package.
- The performance with the MSM detectors should be studied in greater depth.

6. Appendices

6.1 Confinement factor- Mathematica Platform

```
"Even modes";
Eeyi = B * Cos[h * x] Cos[w * t - β * z];
Eeyo = A * Exp[-p * (Abs[x] - d)] Cos[w * t - β * z];
"Odd modes";
Eoyi = B * Cos[h * x] Cos[w * t - β * z];
Eoyo = A * Exp[-p * Abs[x] - d] Cos[w * t - β * z];
"FINDING THE ROOTS TO SOLVE MAXWELL EQUATION";
λ0 = 1650 * 10^-9; "μm";
d = 220 * 10^-9; "thickness";
k0 = 2 π / λ0 ;
η2 = 3.476; "Si";
η1 = 1.442; "SiO2";
η3 = 1.455; "Biodiesel";
v = √((η2 - η1)^2 k0^2 d^2);
v1 = √((η2 - η3)^2 k0^2 d^2); "v="
v
v1
x1[hd_] = √(v^2 - hd^2); "=pd";
x2[hd_] = hd * Tan[hd];
x3[hd_] = -hd * Cot[hd];
"Roots for solving Maxwell equations"
Plot[{x1[t], x2[t], x3[t]}, {t, 0, v},
 PlotStyle → {{RGBColor[0, 0, 1]}, {RGBColor[1, 0, 0]},
   {RGBColor[0, 1, 0]}} , PlotRange → {0, v},
 Frame → True,
 FrameLabel →
  {StyleForm["hd", FontSize → 16, FontFamily → Arial],
                  StyleForm["pd", FontSize → 14,
```

```
    FontFamily → Arial]}]
"This Root is tha value to put in a:"
FindRoot[√(v^2 - hd^2) == hd * Tan[hd], {hd, .7}]
"#################################################";
x4[u_] = √(v1^2 - u^2);
x5[u_] = u * Tan[u];
x6[u_] = -u * Cot[u];
"Roots for solving Maxwell equations";
"Plot[{x4[t],x5[t],x6[t]},{t,0,v1},PlotStyle→
    {{RGBColor[0,0,1]},{RGBColor[1,0,0]},
    {RGBColor[0,1,0]}} ,PlotRange→{0,v1},Frame→
    True,FrameLabel→{StyleForm[" hd
  ",FontSize→16,FontFamily→Arial],StyleForm["
  pd ",FontSize→14,FontFamily→Arial]}]";
"This Root is tha value to put in a1:"
FindRoot[√(v1^2 - hd1^2) == hd1 * Tan[hd1], {hd1, .7}]

"Single mode waveguide TE00"
"################################################
   #########";
"#####If d is changed replace the last value in
   a#####";
"################################################
   #######";
a = 0.8940313320456533`;
a1 = 0.8913162878355906`;
pd = √(v^2 - a);
```

```
f1 = Sqrt[v1^2 - a1];
h = a / d;
p = pd / d;
l1 = f1 / d;
p7 = Plot3D[Exp[-p * (Abs[x] - d / 2)] Cos[z],
    {x, -5 d, -d / 2}, {z, 0, 4 π}, PlotPoints → 40,
    Mesh → False];
p8 = Plot3D[1 / Cos[h * d / 2] Cos[h * x] Cos[z],
    {x, -d / 2, d / 2}, {z, 0, 4 π}, PlotPoints → 40,
    Mesh → False];
p9 = Plot3D[Exp[-p * (Abs[x] - d / 2)] Cos[z],
    {x, d / 2, 5 d}, {z, 0, 4 π}, PlotPoints → 40,
    Mesh → False];
Show[{p7, p8, p9}]
"Cosidering z=0 and t=0";
p1 = Plot[(1 / Cos[h * d / 2] Cos[h * x])^2, {x, -d / 2, d / 2},
    PlotStyle → {RGBColor[0, 0, 1]}];
p2 = Plot[Exp[-l1 * (Abs[z] - d / 2)]^2, {z, d / 2, 3 d},
    PlotStyle → {{RGBColor[0, 1, 0]}}];
p3 = Plot[Exp[-p * (Abs[x] - d / 2)]^2, {x, -3 d, -d / 2},
    PlotStyle → {{RGBColor[1, 0, 0]}}];
Show[{p1, p2, p3}, GridLines → {{-d / 2, d / 2}, None},
  Frame → True,
  FrameLabel → {"Widht [m]", "Intensity [A.U.]"},
  RotateLabel → True];
A = ∫_(-d/2)^(d/2) (1 / Cos[h * d / 2] Cos[h * x])^2 dx +
    ∫_(-∞)^(-d/2) Exp[-p * (Abs[x] - d / 2)]^2 dx;
Abio = ∫_(d/2)^∞ Exp[-l1 * (Abs[x] - d / 2)]^2 dx;

"Porcentage Modes Values Outside Vs Inside";
Γi = Abio / A * 100;
"Value for the confinement factor in the region
  to add the biodiesel:Γ="
(Γi) "%"
```

7. References

[1] A. Casas Bedoya, M.Y. Ling, J. Brouckaert, N.A Yebo, D. Van Thourhout, R. Baets. Biodiesel sensing using Silicon-on-Insulator technologies. Proc of SPIE, 2009. - Vol. 7366-12.

[2] N. D. Mortimer P. Cormack, M. A. Elsayed and R. E. Horne. Evaluation of the comparative energy, global warming and socio-economic cost and benefits of Biodiesel [Book]. Sheffield Resources research unit school of environment and development, 2003.

[3] Ling Meng Yee Design and fabrication of a near-infrared spectroscopy system for sensing applications [Book]. Erasmus Mundus M.Sc.in Photonics Thesis, 2008.

[4] Maria Fernanda Pimentela Grece M.G.S. Ribeiro , Rosenira S. da Cruz , Luiz Stragevitch, José Geraldo. Pacheco Filho, Leonardo S.G. Teixeira Determination of Biodiesel content when blended with mineral Diesel fuel using infrared spectroscopy and multivariate calibration [Journal]. Microchemical Journal, 2006. - Vol. 82. pp. 201-206.

[5] Knothe Gerhard Rapid Monitoring of Transesterification and Assessing Biodiesel Fuel Quality by Near-Infrared Spectroscopy Using a Fiber-Optic Probe [Journal]. JAOCS, 1999. - Vol. 76.

[6] Rosane Falate Karen Nike and Pedro Ramos da Costa Neto, Eduardo Cação Jr., Marcia Muller, Hypolito José Kalinowski and José Luís Fabris Alternative technique for biodiesel quality control using an optical fiber long period [Journal]. - Curitiba – PR : Quim. Nova, 2007. Vol. 30. pp. 1677-1680.

[7] W. H. Wang Y. Z. Tang, Y. X. Wang, H. C. Qu, Y. M. Wu, T. Li, J. Y. Yang, Y. L. Wang, and M. Liu Etched-diffraction-grating-based planar waveguide demultiplexer on silicon-on-insulator [Journal]. - : Opt. Quantum Electronics, 2004. Vol. 36. pp. 559 -566.

[8] J. Brouckaert G. Roelkens, S. Selvaraja, W. Bogaerts, P. Dumon, S. Verstuyft, Z. Yu, D. Van Thourhout, R. Baets. Miniature Integrated Spectrometer Fabricated on a Silicon-on-Insulator Substrate [Journal]. United States: Leos Annual Meeting, 2008.

[9] Joost Brouckaert Wim Bogaerts, Pieter Dumon, Dries Van Thourhout, Roel Baets. Planar Concave Grating Demultiplexer With Hight Reflective Bragg Reflector Facets [Journal]. - Gent : IEEE Photonics technology letters, 2008. Vol. 20. pp. 309-311.

[10] Joost Brouckaert Gunther Roelkens, Dries Van Thourhout, and Roel Baets Thin-Film III–V Photodetectors Integrated on Silicon-on-Insulator Photonic ICs [Journal]. - Gent : IEEE Journal of lightwave technology, 2007. Vol. 25.

[11] http://www.photond.com/products/fimmwave/fimmwave2.htm. FIMMWAVE. - 2008.

[12] CAMFR. - 2008. http://camfr.sourceforge.net/index.html.

[13] Dumon Pieter Ultra-compact integrated optical filtes in Silicon-on-insulator by means of wafer-scale technology [Book]. Univerisitet Gent, 2007.

[14] Taillaert Dirk Grating Couplers as Interface between Optical Fibres and Nanophotonic Waveguides [Book]. Gent University, 2004. Doctoral Thesis.

[15] Wolfram Mathematica / ed. http://www.wolfram.com/.

[16] Joost Brouckaert Wim Bogaerts, Pieter Dumon, Dries Van Thourhout, and Roel Baets Planar Concave Grating Demultiplexer Fabricated on a Nanophotonic Silicon-on-Insulator Platform [Journal]. - Gent : IEEE Journal of lightwave technology, 2007. Vol. 25. - pp. 1269-1274.

[17] J. Brouckaert W. Bogaerts, S. Selvaraja, P. Dumon, R. Baets, and D. Van Thourhout Planar Concave Grating Demultiplexer With High Reflective Bragg Reflector Facets [Journal]. - 2008 : IEEE photonics technology letters, Gent. Vol. 20. - pp. 309-311.

[18] McGreer M. S. D. Smith and K. A. Diffraction gratings utilizing total internal reflection facets in littrow configuration [Journal]. IEEE Photon. Technol. Lett, 1999. Vol. 11. - pp. 84–86.

[19] S. Selvaraja Patrick Jaenen, Stephan Beckx, W. Bogaerts, P. Dumon, D. Van Thourhout, R. Baets Silicon nanophotonic wire structures fabricated by 193nm optical lithography [Journal]. Proc of SPIE, 2008. - Vol. 7134.

[20] Q. Xu V. R. Almeida, R. R. Panepucci, and M. Lipson Experimental demonstration of guiding and confining light in nanometer-size low-refractive-index materia [Journal]. Opt. Lett, 2004. - 14 : Vol. 29. - pp. 1626-1628.

[21] Gunther Roelkens Joost Brouckaert, Steven Verstuyft, Jonathan Schrauwen, Dries Van Thourhout and Roel Baets Heterogeneous integration of III-V photodetectors and laser diodes on silicon-on-insulator waveguide circuits. 3rd IEEE International Conference, 2006. pp. 188-190.

[22] Bogaerts Wim The dummy's guide to mask designing with IPKISS/PICAZZO: by and for dummies. - Gent , 2008.

[23] Bogaerts Wim Silicon Photonics. - Stockholm : Erasmus Mundus Master in Photonics summer school, 2008.

[24] Arthur Nitkowski Long Chen, Michal Lipson. Cavity-enhanced on-chip absorption spectroscopy using microring resonators [Journal]. Ithaca, NY : Optics express, 2008. - 16 : Vol. 16. - pp. 11930-11936.